

On the risks of using double precision in numerical simulations of spatio-temporal chaos

Tianli Hu^a, Shijun Liao^{a,b,c,d,*}

^a Center of Advanced Scientific Computing, School of Naval Architecture, Ocean and Civil Engineering, Shanghai Jiao Tong University, China

^b State Key Laboratory of Ocean Engineering, Shanghai 200240, China

^c State Key Laboratory of Plateau Ecology and Agriculture, Xining 810018, China

^d School of Hydraulic and Electric Engineering, Qinghai University, Xining 810018, China



ARTICLE INFO

Article history:

Received 18 October 2019

Received in revised form 20 May 2020

Accepted 30 May 2020

Available online 10 June 2020

Keywords:

Spatio-temporal chaos

Reliable simulation

Numerical noise

ABSTRACT

Due to the butterfly-effect, computer-generated chaotic simulations often deviate exponentially from the true solution, so that it is very hard to obtain a reliable simulation of chaos in a long-duration time. In this paper, a new strategy of the so-called Clean Numerical Simulation (CNS) in physical space is proposed for spatio-temporal chaos, which is computationally much more efficient than its predecessor (in spectral space). The strategy of the CNS is to reduce both of the truncation and round-off errors to a specified level by implementing high-order algorithms in multiple-precision arithmetic (with sufficient significant digits for all variables and parameters) so as to guarantee that numerical noise is below such a critical level in a temporal interval $t \in [0, T_c]$ that corresponding numerical simulation remains reliable over the whole interval. Without loss of generality, the complex Ginzburg-Landau equation (CGLE) is used to illustrate its validity. As a result, a reliable long-duration numerical simulation of the CGLE is achieved in the whole spatial domain over a long interval of time $t \in [0, 3000]$, which is used as a reliable benchmark solution to investigate the influence of numerical noise by comparing it with the corresponding ones given by the 4th-order Runge-Kutta method in double precision (RK4D). Our results demonstrate that the use of double precision in simulations of chaos might lead to huge errors in the prediction of spatio-temporal trajectories and in statistics, not only quantitatively but also qualitatively, particularly in a long interval of time.

© 2020 Elsevier Inc. All rights reserved.

1. Introduction

In 1890 Poincaré [1] discovered that the trajectories of an N -body system ($N \geq 3$), governed by Newtonian gravitational attraction, generally have sensitive dependence on the initial condition (SDIC), i.e. a tiny difference in initial condition might lead to a completely different trajectory. The so-called SDIC was rediscovered in 1963 by Lorenz [2] who numerically solved an idealized model of weather prediction, nowadays called the Lorenz equation, by means of a digital computer. The SDIC became popularized following the title of a talk in 1972 by Lorenz to the American Association for the Advancement of Science as “Does the flap of a butterfly’s wings in Brazil set off a tornado in Texas?”. In his seminal paper, Lorenz stated

* Corresponding author at: Center of Advanced Scientific Computing, School of Naval Architecture, Ocean and Civil Engineering, Shanghai Jiao Tong University, China.

E-mail address: sjliao@sjtu.edu.cn (S. Liao).

that “long-term prediction of chaos is impossible” [2]. The discovery of Poincaré [1] and Lorenz [2] has helped create a completely new field in science, called chaos theory.

Furthermore, Lorenz [3,4] found that computer-generated simulations of a chaotic dynamic system using the Runge-Kutta method in the *double* precision are sensitive *not only* to the initial condition *but also* to the numerical algorithms (including temporal/spatial discretization). For the specific problem investigated, Lorenz [4] reported that the Lyapunov exponent, one of the most important characteristics of a dynamic system, frequently varied its sign even when the time-step became rather small. It is well-known that only a positive Lyapunov exponent corresponds to chaos; a negative one does not! This is easy to understand from the viewpoint of the so-called butterfly-effect, because numerical noise from truncation and round-off error is *unavoidable* in *any* numerical simulation, and leads to some errors (or approximations) being introduced to the solution at each time-step. For example, let us consider the high-order Taylor expansion

$$f(t + \Delta t) \approx f(t) + \sum_{m=1}^M \frac{f^{(m)}(t)}{m!} (\Delta t)^m, \quad (1)$$

where $f(t)$ is a function of time t , Δt is the time-step, M is the order of Taylor expansion and $f^{(m)}(t)$ is the m th-order derivative of $f(t)$. Given that M is *finite* in practice, we obtain a truncation error as the difference between the results of the infinite and truncated Taylor series. Moreover, because all variables and physical/numerical parameters, such as $f(t)$, $f^{(m)}(t)$, Δt and so on, are expressed in a precision (usually double precision) limited by a *finite* number of significant digits, a round-off error invariably arises. Logically, a chaotic system with the butterfly-effect should also be rather sensitive to these *man-made* numerical errors. This kind of sensitive dependence on numerical algorithm (SDNA) for a chaotic system has been confirmed by many researchers [5–7], and has led to some intense arguments and serious doubts concerning the reliability of numerical simulations of chaos. It has even been hypothesized that “all chaotic responses are simply numerical noise and have nothing to do with the solutions of differential equations” [8]. Note that the foregoing researchers [5–8] undoubtedly used data in *double* precision for chaotic systems, although different types of numerical algorithm were tested. As a consequence, it was not clear how numerical noise influenced the reliability of numerical simulations of chaos.

Without doubt, the reliability of computer-generated simulation of chaotic systems is a very important fundamental problem. Anosov [9] in 1967 and Bowen [10] in 1975 showed that *uniformly hyperbolic* systems have the so-called shadowing property: a computer-generated (or noisy) orbit will stay close to (shadow) true orbits with *adjusted* initial conditions for arbitrarily long times. Let $\{\mathbf{p}_k\}_{k=a}^b$ denote a δ_f -pseudo-orbit for \mathbf{f} if $|\mathbf{p}_{k+1} - \mathbf{f}(\mathbf{p}_k)| < \delta_f$ for $a < k < b$, where \mathbf{f} is a D -dimensional map and \mathbf{p} is a D -dimensional vector representing the dynamical variables. Here the term pseudo-orbit is used to describe a computer-generated noisy orbit. The true orbit $\{\mathbf{y}_k\}_{k=a}^b$ δ -shadows $\{\mathbf{p}_k\}_{k=a}^b$ on $[a, b]$ if $|\mathbf{y}_k - \mathbf{p}_k| < \delta$, where the true orbit $\{\mathbf{y}_k\}_{k=a}^b$ satisfies $\mathbf{y}_{k+1} = \mathbf{f}(\mathbf{y}_k)$. For details of the shadowing theorems, please refer to [9–14].

However, hardly any chaotic systems are uniformly hyperbolic. Dawson et al. [15] pointed out that the non-existence of such shadowing trajectories may be caused by finite-time Lyapunov exponents of a system fluctuating about zero. For non-hyperbolic chaotic systems with unstable dimension variability, no true trajectory of reasonable length can be found to exist near any computer-generated trajectories, as reported by Do and Lai [16]. Using examples having only two degrees of freedom, Sauer [17] showed that extremely small levels of numerical noise might result in macroscopic errors even in simulation average *statistics* that are several orders of magnitude larger than the noise level. Thus, the good promise from the Shadow Lemma [9,10] for a uniformly hyperbolic system does not work for many non-hyperbolic systems [18]. It seems that we had to be satisfied with finite-length shadows for non-hyperbolic systems [19]. Note that most of investigations on shadows are based on low dimensional dynamic systems, although a shadowing algorithm for high dimensional systems (such as the motion of one hundred stars) was proposed by Hayes and Jackson [19]. To the best of our knowledge, neither rigorous shadowing theorems nor practical shadowing algorithms have been proposed for spatio-temporal chaotic systems (such as turbulent flows), which are governed by nonlinear PDEs and thus have an infinite number of dimensions. It seems that, although the shadowing concept is rigorous in mathematics, it is hardly used in practice for complicated systems such as spatio-temporal chaos and turbulence that are non-hyperbolic in general and besides have an infinite number of degrees of freedom.

Liao [20–22] suggested a numerical strategy called “Clean Numerical Simulation” (CNS) that could provide reliable simulations of chaotic systems over a given finite interval of time. The CNS is based on an *arbitrary*-order Taylor expansion method [23–27], multiple-precision (MP) data [28] with *arbitrary* numbers of significant digits, and a solution verification check [29,30] (using another simulation for the same physical parameters but with even smaller numerical noise). Here, the word “arbitrary” means a value which can be “as large as required”. So, as long as the order M of the Taylor expansion (1) is *sufficiently* large and all data values are expressed in multiple-precision with a *sufficiently* large number of significant digits (denoted by N_s), both the truncation error and the round-off error can be held below specified thresholds throughout a prescribed simulation time $[0, T_c]$. Here the so-called critical predictable time T_c is determined through the solution verification check by comparing it to an additional simulation with the same physical parameters but smaller numerical noise, such that the difference between them remains negligible in the interval $[0, T_c]$. Thus, a basic task of the CNS is to determine the relationship between T_c and numerical noise. This relationship needs clarification particularly as it has been largely ignored by researchers working on chaotic dynamics.

The CNS is based on such a hypothesis that the level of numerical noise increases exponentially (in an average meaning) within an interval of time $t \in [0, T_c]$, say,

$$\mathcal{E}(t) = \mathcal{E}_0 \exp(\mu t), \quad t \in [0, T_c], \quad (2)$$

where the constant $\mu > 0$ is the so-called “noise-growing exponent” that is dependent upon the physical parameters of the system, \mathcal{E}_0 denotes the level of initial noise (i.e. truncation and round-off error), $\mathcal{E}(t)$ is the level of evolving noise of the computer-generated simulation at the time t , respectively. The critical predictable time T_c is determined by a critical level of noise \mathcal{E}_c , say,

$$\mathcal{E}_c = \mathcal{E}_0 \exp(\mu T_c), \quad (3)$$

which gives

$$T_c = \frac{(\ln \mathcal{E}_c - \ln \mathcal{E}_0)}{\mu}. \quad (4)$$

So, for a given critical level of noise \mathcal{E}_c , the smaller the level of the initial noise \mathcal{E}_0 , the larger the critical predictable time of T_c .

However, it is practically impossible to exactly calculate the level of evolving noise $\mathcal{E}(t)$, because the true solution is unknown. So, we should propose a practical method with sufficiently high accuracy to determine T_c . Let $\mathbf{x} \in \Omega$ denote a vector of spatial coordinates and $\psi(\mathbf{x}, t)$ a computer-generated simulation reliable in $t \in [0, T_c]$ with the level of initial noise \mathcal{E}_0 , $\psi'(\mathbf{x}, t)$ is another computer-generated simulation reliable in $t \in [0, T'_c]$ with a level of initial noise \mathcal{E}'_0 that is several orders of magnitude smaller than \mathcal{E}_0 . According to the hypothesis of exponential growth in numerical noise of chaotic systems, it holds that $T'_c > T_c$ and $\psi'(\mathbf{x}, t)$ in $t \in [0, T_c]$ should be much closer to the true solution than $\psi(\mathbf{x}, t)$ and thus can be regarded as a *reference* to approximately calculate the level of numerical noise of $\psi(\mathbf{x}, t)$ in $\mathbf{x} \in \Omega$. Note that a similar idea was used by Turchetti et al. [31] who compared a numerical map computed for a given accuracy (single floating-point precision) with the same map evaluated numerically with a higher accuracy (double or higher floating-point precision) that is regarded as the reference map. In practice, the value of T_c can be determined by comparing $\psi(\mathbf{x}, t)$ with another better simulation $\psi'(\mathbf{x}, t)$ having smaller initial noise \mathcal{E}'_0 . In this way, the level of numerical noise of $\psi(\mathbf{x}, t)$ is not beyond the critical level \mathcal{E}_c of noise in the temporal interval $t \in [0, T_c]$ within the whole spatial domain $\mathbf{x} \in \Omega$. In other words, $\psi(\mathbf{x}, t)$ is a “clean” numerical simulation (CNS) in $t \in [0, T_c]$ and $\mathbf{x} \in \Omega$. The above-mentioned can be regarded as a heuristic explanation of the strategy of the CNS.

Liao [20] successfully used this strategy of the CNS to gain reliable chaotic simulations of the Lorenz equation and indeed found that the smaller the numerical noise, the larger the value of T_c . Liao also found that when the data are of high multiple-precision, such that N_s is sufficiently large for round-off errors to be ignored and the truncation error dominates, T_c is linearly proportional to M , the order of Taylor expansion. Moreover, when M reaches such a sufficiently high value that round-off error dominates, then T_c becomes linearly proportional to N_s , the number of significant digits. Using these linear relationships, it is possible to determine values for M and N_s that apply to *any* prescribed T_c . Here, T_c is finite due to computer limitations, but can be quite large, depending on the computer resources available. For example, Liao [20] applied CNS to obtain a reliable chaotic simulation of Lorenz equation until $T_c = 1000$ Lorenz time unit (LTU) by means of $\Delta t = 0.01$, $M = 400$ and $N_s = 800$. Furthermore, Liao and Wang [32] used the CNS to obtain, for the first time, a convergent/reliable chaotic simulation of Lorenz equation up to $T_c = 10000$ LTU by means of $M = 3500$ and $N_s = 4180$, using 1200 CPUs to the National Supercomputer TH-1A in Tianjin, China. Note that the reliability of this long-term chaotic simulation was verified by means of another better simulation using $M = 3600$ and $N_s = 4515$. These showed the validity of the CNS. Note that, exactly for the same physical parameters and the same initial conditions of the Lorenz equation, by means of the 4th-order Runge-Kutta’s method and many other algorithms in *double* precision, a reliable chaotic simulation is often obtained over a rather small interval, approximately $[0, 30]$ LTU, which is only 0.3% of the interval $[0, 10000]$. This may be the underlying reason why there is such controversy about the reliability of numerical simulations of chaos [8], noting that most researchers neglect the influence of round-off error and use *double* precision in their computer-generated simulations.

In CNS, numerical noise arising from truncation and round-off errors is much smaller than the values of physical variables under consideration, provided $t < T_c$, where T_c is a specified parameter that can be as large as deemed necessary by the user. Consequently, many complicated chaotic systems can be studied by means of the CNS, as illustrated in [33–39]. For example, according to Poincaré [1], a three-body system can often be chaotic. In physics, the initial positions of the three-bodies have inherent micro-level physical uncertainty, at scales below the Planck length scale. Such micro-level uncertainty in the initial position is much smaller than the round-off error caused by the use of double precision, and so its influence on macroscopic trajectories cannot be investigated by traditional algorithms using double precision arithmetic. However, using CNS, Liao and Li [35] investigated the propagation of micro-level physical uncertainty in the initial condition for a chaotic three-body system, and found that the uncertainty grows to become macroscopic, leading to random escape and symmetry-breaking behaviour of the three-body system. This implies that micro-level physical uncertainty might be the origin of macroscopic randomness in the three-body system. Besides, given that micro-level uncertainty is physically inherent, the

escape and symmetry-breaking behaviour of the chaotic three-body system can happen even *without* any external forces present. In other words, such behaviour is self-excited. This suggests that macroscopic randomness, self-excited random escape, and self-excited symmetry-breaking of a chaotic three-body system are unavoidable. (Liao and Li [35] provide further details.) Notably, although the three-body problem can be traced back to Newton in 1680s, only three families of periodic orbits were found in the 300 years since then. In 1890 Poincaré [1] pointed out that a three-body system is chaotic in general and its closed-form solution does not exist. This is why so few periodic orbits have been discovered. However, by undertaking CNS on China's national supercomputer, Li, Jing and Liao [36,37,39] successfully found more than 2000 new periodic orbits of three-body system. The new periodic orbits were profiled in New Scientists [40,41]. All of these illustrated the usefulness of CNS as a powerful tool for reliable and accurate investigation of chaotic systems in physics.

The Lorenz equation is a greatly simplified form of the Navier-Stokes equations that are widely used to describe turbulent flows. In 2017 Lin et al. [38] applied the CNS to study the relationship between inherent micro-level thermal fluctuation and the macroscopic randomness of a two-dimensional Rayleigh-Bérnard convection turbulent flow in a long enough interval of time, taking micro-level thermal fluctuation (expressed by Gaussian white noise) to be the initial condition, with no external disturbances applied. Using CNS with numerical noise set to be even smaller than the micro-level thermal fluctuations, Lin et al. [38] proved theoretically that inherent micro-level thermal fluctuations are the root source of macroscopic randomness of Rayleigh-Bérnard turbulent convection flows. Unlike the Lorenz system and three-body system, which are described mathematically by ordinary differential equations (ODEs), the Rayleigh-Bérnard convection system is governed by partial differential equations (PDE) as a spatio-temporal chaotic system. This case illustrated the validity of the CNS for reliable simulation of spatio-temporal chaotic systems governed by nonlinear PDEs. However, Lin et al. [38] used a Galerkin-Fourier spectral method with CNS to solve the system in spectral space. This involved mapping the original nonlinear PDE in physical space onto a huge system of nonlinear ODEs in spectral space, proving to be rather time-consuming and impractical on present-day computers for simulation for spatio-temporal chaotic systems.

In this paper, we propose a new strategy that greatly increases the computational efficiency of CNS for spatio-temporal chaotic systems. Without loss of generality, we consider the one-dimensional complex Ginzburg-Landau equation (CGLE) as an example of a spatio-temporal chaotic system, to outline the basic features of the strategy and then illustrate its validity and efficiency. Section 2 describes two CNS algorithms: one in spectral space using the Galerkin-Fourier spectral method; the other in physical space. The performance of these algorithms is compared in terms of computational efficiency, validity, etc. Section 3 discusses the influence of numerical noise on spatio-temporal trajectories and statistics of the chaotic system. Section 4 summarizes the discussions and conclusions.

2. CNS algorithms for spatio-temporal chaos

Spatio-temporal chaos, characterized by irregular behaviour in both space and time, arises when a spatially extended system is driven away from its equilibrium state [42]. The one-dimension complex Ginzburg-Landau equation (CGLE), which describes oscillatory media near the Hopf bifurcation, is commonly used in studies of spatio-temporal chaos [43–52], and is given by

$$A_t = A + (1 + i c_1) A_{xx} - (1 - i c_3) |A|^2 A, \quad (5)$$

subject to the initial condition

$$A(x, 0) = f(x)$$

and the periodic boundary condition

$$A(x, t) = A(x + L, t),$$

where $i = \sqrt{-1}$, A is an unknown complex function, the subscript denotes the partial derivative, t and x denote the temporal and spatial coordinates, c_1 and c_3 are physical parameters, respectively. The CGLE has spatio-temporal chaotic solutions in cases when $c_1 c_3 \geq 1$, corresponding to Benjamin-Feir instability [53]. Depending upon the values of c_1 and c_3 , the CGLE exhibits two distinct chaotic phases, namely “phase chaos” when A is bounded away from zero, and “defect chaos” for $A = 0$ when the phase exhibits singularities [43,45,47,54]. As pointed out by Shraiman et al. [45], the crossover between phase and defect chaos is invertible only when $c_1 > 1.9$. Furthermore, the CGLE solution occupies a bichaos region when $c_1 < 1.9$, where phase chaos and defect chaos coexist. Chaté [55] examined the relation with spatio-temporal intermittency, and defined an intermittency regime where defect chaos and stable plane waves coexist. By considering modulated amplitude waves (MAWs), Bruschi et al. [47] found that the crossover between phase and defect chaos take place when the periods of MAWs are driven beyond their saddle-node bifurcation.

Despite intensive numerical investigations into solutions of the CGLE [43,45,47,55–58] for values of c_1 and c_3 ranging from $L = 500$ to $L = 4000$, the sensitive dependence on initial conditions (SDIC) of the CGLE has made it impossible to obtain reliable, long duration numerical simulations of the spatio-temporal chaotic solution by means of the traditional algorithms using *double* precision arithmetic. Here, we use Clean Numerical Simulation (CNS) to obtain reliable computer-generated simulations in a given specified finite interval of time. Taking the one-dimension complex Ginzburg-Landau equation as an

example, we outline two different CNS algorithms for spatio-temporal chaotic systems: one in spectral space, the other in physical space. We will demonstrate that the latter is computationally much more efficient than the former.

First of all, we temporally expand the unknown complex function A in the CGLE by means of the following high-order Taylor expansion

$$A(x, t + \Delta t) = \sum_{m=0}^M A^{[m]}(x, t) (\Delta t)^m, \tag{6}$$

where Δt is the time step, the order M is a (sufficiently large) positive integer, and

$$A^{[m]}(x, t) = \frac{1}{m!} \frac{\partial^m A(x, t)}{\partial t^m}. \tag{7}$$

Note that $|A|^2 = \bar{A} A$, where \bar{A} is the complex conjugate of $A(x, t)$. From Eqs. (5) and (7), we have

$$\begin{aligned} A^{[m]}(x, t) &= \frac{1}{m} A^{[m-1]}(x, t) + \frac{(1 + i c_1)}{m} A_{xx}^{[m-1]}(x, t) \\ &\quad - \frac{(1 - i c_3)}{m} \sum_{j=0}^{m-1} \sum_{n=0}^{m-1-j} \bar{A}^{[j]}(x, t) A^{[n]}(x, t) A^{[m-1-j-n]}(x, t). \end{aligned} \tag{8}$$

Note that $A^{[m]}(x, t)$ is solely dependent upon $A^{[n]}(x, t)$ and its spatial derivative $A_{xx}^{[n]}(x, t)$, where $0 \leq n \leq m - 1$, and thus can be calculated consecutively, up to a high-enough order M ensuring that the truncation error does not exceed a prescribed level. Hence, $A(x + \Delta t)$ is calculated to a required precision, provided the spatial derivative term $A_{xx}^{[n]}(x, t)$ is calculated to sufficient accuracy. This is a key to using the CNS in problems involving spatio-temporal chaos.

2.1. The CNS algorithm in spectral space

In CNS combined with a Galerkin Fourier spectral method, the unknown complex function A of Eq. (5) is expressed by Fourier series (see e.g. Finlayson et al. and Isaacson et al. [59,60]), as follows

$$A(x, t) \approx \sum_{k=-\frac{N}{2}}^{\frac{N}{2}-1} a_k(t) \varphi_k(x), \tag{9}$$

where N is the mode number of the spatial Fourier expansion with the base function

$$\varphi_k(x) = \frac{1}{\sqrt{L}} e^{ik\alpha x}. \tag{10}$$

Here $\alpha = 2\pi/L$, and L is the spatial period of the solution. Then, according to (7),

$$A^{[m]}(x, t) \approx \sum_{k=-N/2}^{N/2-1} a_k^{[m]}(t) \varphi_k(x). \tag{11}$$

After transformation, Eq. (8) becomes

$$\begin{aligned} \int_0^L A^{[m]}(x, t) \bar{\varphi}_k(x) dx &= \frac{1}{m} \int_0^L A^{[m-1]}(x, t) \bar{\varphi}_k(x) dx \\ &+ \frac{(1 + i c_1)}{m} \int_0^L A_{xx}^{[m-1]}(x, t) \bar{\varphi}_k(x) dx \\ &- \frac{(1 - i c_3)}{m} \sum_{j=0}^{m-1} \sum_{n=0}^{m-1-j} \int_0^L \bar{A}^{[j]}(x, t) A^{[n]}(x, t) A^{[m-1-j-n]}(x, t) \bar{\varphi}_k(x) dx, \end{aligned} \tag{12}$$

where $\bar{\varphi}_k(x)$ is the complex conjugate of the basis function $\varphi_k(x)$. Substituting (11) into the above equation, we have for $m \geq 1$ that

$$\begin{aligned}
a_k^{[m]}(t) = & \frac{1}{m} a_k^{[m-1]}(t) - \frac{(1 + i c_1)}{m} \left(\frac{2k\pi}{L} \right)^2 a_k^{[m-1]}(t) \\
& - \frac{(1 - i c_3)}{mL} \sum_{-k_1+k_2+k_3=k} \sum_{j=0}^{m-1} \sum_{n=0}^{m-1-j} \bar{a}_{k_1}^{[j]}(t) a_{k_2}^{[n]}(t) a_{k_3}^{[m-1-j-n]}(t), \\
& -\frac{N}{2} \leq k, k_1, k_2, k_3 \leq \frac{N}{2} - 1,
\end{aligned} \tag{13}$$

where $\bar{a}_k^{[n]}(t)$ is the complex conjugate of $a_k^{[n]}(t)$, with $a_k^{[0]}(t) = a_k(t)$ and $\bar{a}_k^{[0]}(t) = \bar{a}_k(t)$. The initial condition of $a_k(t)$ is given by

$$a_k(0) = \int_0^L A(x, 0) \bar{\varphi}_k(x) dx, \quad -\frac{N}{2} \leq k \leq \frac{N}{2} - 1. \tag{14}$$

In the frame of CNS, we apply the temporal high-order Taylor expansion

$$a_k(t + \Delta t) \approx \sum_{m=0}^M a_k^{[m]}(t) (\Delta t)^m, \quad -\frac{N}{2} \leq k \leq \frac{N}{2} - 1, \tag{15}$$

subject to the initial condition (14), to decrease the truncation error to a required level. We also ensure that calculations are performed in multiple-precision using a sufficient number N_s of significant digits to limit the round-off error to below a specified level, and carry out a verification check on the solution by considering results from an additional simulation with even smaller numerical noise to determine the critical predictable time T_c . Here $a_k^{[m]}(t)$ is given by (13), Δt is the time step, M is the order of the Taylor expansion, and N is the mode number of the spatial Fourier expansion, respectively. So long as all values of $a_k(t)$ in spectral space are known, the solution $A(x, t)$ can be determined in physical space by means of (9), as and when required. As mentioned in the Introduction, this CNS algorithm in spectral space was successfully used by Lin et al. [38] to study the influence of inherent micro-level thermal fluctuations on the macroscopic randomness of turbulent Rayleigh-Bernard turbulent convection. Lin et al. found that the accuracy of this Galerkin Fourier spectral method is very high, provided N , M , and N_s are all sufficiently large. However, as reported by Lin et al. [38], calculation of the nonlinear term in (13) is very time consuming when N is large.

2.2. The CNS algorithm in physical space

To overcome the shortcoming of the above-mentioned CNS algorithm in spectral space, we propose the following CNS algorithm in physical space. Instead of mapping the original governing equation and initial condition onto spectral space, via a collocation method [61,62], we directly solve the original equation in physical space by first dividing the spatial domain $[0, L]$ into a uniform grid, such that

$$x_k = \frac{kL}{N} = k\Delta x, \quad k = 0, 1, 2, 3, \dots, N,$$

and then approximating $A(x, t)$ by a set of discrete unknown variables

$$\{A(x_0, t), A(x_1, t), A(x_2, t), \dots, A(x_N, t)\}, \tag{16}$$

where $A(x_N, t) = A(x_0, t)$ in order to satisfy the periodic condition. Thus, we have only N unknowns $A(x_k, t)$ ($0 \leq k \leq N-1$), whose temporal evolution is given by the high-order Taylor expansion

$$A(x_k, t + \Delta t) \approx \sum_{m=0}^M A^{[m]}(x_k, t) (\Delta t)^m, \quad k = 0, 1, 2, \dots, N-1, \tag{17}$$

where Δt is the time step, and $A^{[m]}(x_k, t)$ defined by (7) is given by

$$\begin{aligned}
A^{[m]}(x_k, t) = & \frac{1}{m} A^{[m-1]}(x_k, t) + \frac{(1 + i c_1)}{m} A_{xx}^{[m-1]}(x_k, t) \\
& - \frac{(1 - i c_3)}{m} \sum_{j=0}^{m-1} \sum_{n=0}^{m-1-j} \bar{A}^{[j]}(x_k, t) A^{[n]}(x_k, t) A^{[m-1-j-n]}(x_k, t),
\end{aligned} \tag{18}$$

with the specified initial condition $A(x_k, 0) = f(x_k)$.

Note that there exists the spatial partial derivative $A_{xx}^{[n]}(x_k, t)$ in (18), where $0 \leq n \leq m - 1$ and $0 \leq k \leq N - 1$ are positive integers. To evaluate accurately this spatial partial derivative term from the set of the known discrete variables $A^{[n]}(x_j, t)$, we first invoke the Fourier expansion in space,

$$A^{[n]}(x, t) \approx \sum_{k=-\frac{N}{2}}^{\frac{N}{2}-1} b_k^{[n]}(t) e^{ik\alpha x}, \tag{19}$$

where $\alpha = 2\pi/L$ and

$$b_k^{[n]}(t) \approx \frac{1}{N} \sum_{j=0}^{N-1} A^{[n]}(x_j, t) e^{-ik\alpha x_j}, \quad -\frac{N}{2} \leq k \leq \frac{N}{2} - 1. \tag{20}$$

This is given by the set of the known variables $A^{[n]}(x_j, t)$ at discrete points x_j ($0 \leq j \leq N - 1$). Then, we have the spatial partial derivative term

$$A_{xx}^{[n]}(x_j, t) \approx -\alpha^2 \sum_{k=-\frac{N}{2}}^{\frac{N}{2}-1} k^2 b_k^{[n]}(t) e^{ik\alpha x_j}, \quad 0 \leq j \leq N - 1, \tag{21}$$

where $b_k^{[n]}(t)$ is given by (20). The Fast Fourier Transform (FFT) [63] is used to increase computational efficiency, given that the discrete points x_j are equidistant.

Obviously, the larger the order M of the Taylor expansion (17) in time and the mode number N of the Fourier expansion (19) in space, the smaller the corresponding truncation errors. To decrease the round-off error to a required level, all variables and physical parameters are calculated in multiple-precision with N_s significant digits, where N_s is a sufficiently large positive integer. In this way, both the truncation and round-off errors are reduced to a required limiting level. Finally, an additional numerical simulation with smaller numerical noise is carried out to determine the critical predictable time T_c (i.e. the maximum time of reliable simulation) by comparing the results of both simulations; this ensures that the CNS result is reliable within the temporal interval $t \in [0, T_c]$ over the whole spatial domain.

Comparing (18) with (13), it is obvious that the CNS algorithm in physical space is numerically much more efficient than the CNS algorithm in spectral space, especially for a large mode number N of the spatial Fourier expansion. This is indeed true, as shown in §2.5.

Note that the high order Taylor expansion method [23–27], the Fourier expansion method [63], the multiple precision [28], and the solution verification check [29,30] are widely used. However, their combination may give reliable simulations of spatio-temporal chaotic systems, which provide us benchmarks that can be used to study the influence of numerical noise on chaotic simulations given by traditional algorithms in double precision.

2.3. The optimal time-step

In CNS, the temporal truncation error is determined by the order M of the Taylor expansion (15) or (17), and the spatial truncation error is determined by the mode number N of the spatial Fourier expansion (9) or (19). As long as both M and N are large enough, the temporal and spatial truncation errors are reduced to below a target level. In addition, the round-off error is reduced to a specified level by using multiple-precision with sufficiently large number N_s of significant digits.

To calculate the M th-order Taylor expansion (15) or (17) in time dimension, we use an optimal time-step [27]

$$\Delta t = \min \left(\frac{g(tol, M - 1)}{\|A^{(M-1)}(x_k, t)\|_{\infty}^{1/(M-1)}}, \frac{g(tol, M)}{\|A^{(M)}(x_k, t)\|_{\infty}^{1/M}} \right), \tag{22}$$

where tol is an allowed tolerance at each time step, $\|A^{(M)}(x_k, t)\|_{\infty}$ is the infinite norm of the M th-order Taylor expansion of the modules of $A(x_k, t)$, $k = 0, 1, 2, 3, \dots, N - 1$ and

$$g(tol, M) \approx tol^{1/(M+1)}. \tag{23}$$

To save computer resources and increase computational efficiency, it is reasonable to enforce the allowed tolerance to be at the same level as the round-off error, say,

$$tol = 10^{-N_s}. \tag{24}$$

Thus, we have the optimal time-step as

$$\Delta t = \min \left(\frac{10^{-N_s/M}}{\|A^{(M-1)}(x_k, t)\|_{\infty}^{1/(M-1)}}, \frac{10^{-N_s/(M+1)}}{\|A^{(M)}(x_k, t)\|_{\infty}^{1/M}} \right). \tag{25}$$

Therefore, for a given number N_s of significant digits in multiple-precision, one has the freedom to choose the order M of temporal Taylor expansion. According to (25), raising the order of the temporal Taylor expansion usually leads to an increased optimal time-step Δt . So, in practice, it makes sense to set M to higher order because it can also improve the speed-up ratio of the parallelized algorithm.

In practice, we first choose a sufficiently large values for N_s and M to meet the error requirements, from which the optimal time-step Δt is evaluated by (25) at each time-step. In this way, the temporal truncation error is kept to the same level of the round-off error.

For a spatio-temporal chaotic system (5), it is also necessary to limit the spatial truncation error, determined by the mode number N of the spatial Fourier expressions (9) or (19). Obviously, the larger the value of N , the smaller the spatial truncation error. In theory, to save computer resources and improve computational efficiency, it is better to let the spatial truncation error be equal to the temporal truncation error. Unfortunately, it is presently unknown how to do this. In practice, we often choose reasonably large values for N_s and N in order to guarantee that the round off error, temporal truncation error, and spatial truncation error are *all* below a specified level. Finally, the solution verification check is implemented by comparing the numerical result to that of an additional simulation with even smaller numerical noise; this determines the finite time interval $[0, T_c]$, over which the spatio-temporal chaotic numerical results exhibit no distinct differences at *all* spatial grid-points and thus are reliable.

2.4. Criteria of reliability and convergence

Due to the sensitivity dependence on initial conditions of chaotic systems, unavoidable numerical noise from round-off and truncation errors can increase exponentially. To guarantee the reliability of chaotic numerical simulations, we compare our CNS simulation of interest against one using the same physical parameters and the same algorithm but with even smaller numerical noise; this determines the finite time interval $[0, T_c]$ over which the spatio-temporal chaotic numerical results display no distinct differences at *all* spatial grid-points.

Take the one-dimensional CGLE as an example. Let $A(x, t)$ denote a numerical simulation of the one-dimensional CGLE, given by CNS using the M th-order of Taylor expansion in the time dimension, the mode number N of the Fourier expansion in the spatial dimension, the number N_s of significant digits in the multiple precision scheme. Now, let $A'(x, t)$ be another CNS result with even smaller numerical noise, given by the M' th-order of the temporal Taylor expansion, the mode number N' of the spatial Fourier expansion, and number N'_s of significant digits in the multiple precision scheme, where $M' \geq M$, $N' > N$ and $N'_s \geq N_s$. Since the level of numerical noise increases exponentially, $A'(x, t)$ (with smaller numerical noises) should be closer to the true solution than $A(x, t)$ and thus can be used as a reference solution to check the reliability of $A(x, t)$.

If $A(x, t)$ and $A'(x, t)$ have the same spatial discretization, i.e. the same N , their deviation can be measured by

$$\delta(t) = \frac{\sqrt{\sum_{k=0}^{N-1} |A(x_k, t) - A'(x_k, t)|^2}}{\sqrt{\sum_{k=0}^{N-1} |A'(x_k, t)|^2}}. \quad (26)$$

However, $A'(x, t)$ often has different values of N from $A(x, t)$ in practice. In this case, it is more convenient to compare their spatial spectrum. Rewrite $A(x, t)$ and $A'(x, t)$ in the spatial Fourier expressions

$$A(x, t) \approx \sum_{k=-\frac{N}{2}}^{\frac{N}{2}-1} B_k(t) e^{ik\alpha x}, \quad A'(x, t) \approx \sum_{k=-\frac{N'}{2}}^{\frac{N'}{2}-1} B'_k(t) e^{ik\alpha x}. \quad (27)$$

Note that $\sum_{k=-\frac{N'}{2}}^{\frac{N'}{2}-1} |B'_k|^2$ has often physical meaning, such as the total energy of the system. So, from a physical viewpoint, it is important for a numerical simulation of a spatio-temporal chaos to have an accurate spatial spectrum at given time t . Thus, we define the so-called "spectrum-deviation"

$$\delta_s(t) = \frac{\sum_{k=-\frac{N}{2}}^{\frac{N}{2}-1} \left| |B'_k|^2 - |B_k|^2 \right|}{\sum_{k=-\frac{N'}{2}}^{\frac{N'}{2}-1} |B'_k|^2} \quad (28)$$

Table 1

CPU times of CNS simulations of the one-dimension CGLE for $c_1 = 2$, $c_3 = 1$ and $L = 256$ in the temporal interval $t \in [0, 10]$, in spectral and physical spaces with the same $N_s = 20$, $M = 14$, a fixed time step $\Delta t = 0.01$ and the same mode number N for the spatial Fourier expansion. T_1 and T_2 are the elapsed CPU times for the CNS algorithms in the spectral space; and the physical space, respectively.

N	T_1 (in seconds)	T_2 (in seconds)	T_1/T_2
16	694	7.93	87
32	5530	12.8	432
64	44366	25	1774
128	346490	51	6793

to quantify the difference between $A(x, t)$ and $A'(x, t)$ at a given time t . Obviously, the smaller the spectrum-deviation δ_s , the better the two simulations agree with each other and the greater their reliability. So, it is reasonable to define the reliability criterion as

$$\delta_s < \delta_s^c, \tag{29}$$

where $\delta_s^c > 0$ is a reasonably small number, called the ‘‘critical spectrum-deviation’’. For the problem under consideration, it is found that $\delta_s^c = 0.01$ is reasonable, which is used for all the remaining cases in this paper. Equation (29) provides a criterion of reliability, which determines the so-called ‘‘critical predictable time’’ T_c and the temporal interval $[0, T_c]$, in which the reliability-criteria (29) is satisfied and the differences between the two simulations $A(x, t)$ and $A'(x, t)$ at all spatial grid-points are negligible.

2.5. Computational efficiency of the two CNS algorithms

In theory the CNS algorithm in spectral space undertakes about $O(M^3 N^3)$ elementary operations, whereas the CNS algorithm in physical space undertakes $O(NM \log_2 N + N M^3)$ elementary operations. This is partly due to the fewer nonlinear terms in the right-hand side of (18) than (13), and partly due to the implementation of the FFT in evaluating (21). Obviously, using the CNS algorithm in physical space can greatly improve the calculation speed at $O(N^2)$, where N is the mode number of the spatial Fourier expansion. The resulting speed-up is huge in practice, especially for large N . This is confirmed by the results listed in Table 1 which compares the CPU times taken by the two CNS algorithms, for the same values of N , M , and N_s . For the purposes of comparison, a fixed time-step $\Delta t = 0.01$ is used. Table 1 shows that the ratio T_1/T_2 of required CPU times for the 1st and 2nd CNS algorithms rises exponentially as N increases. Notably, when $N = 128$, the required CPU time of the CNS algorithm in spectral space is 6000 times more than that of the CNS algorithm in physical space! This illustrates that the CNS algorithm in physical space described in Section 2.2 is clearly much more efficient than that in its counterpart spectral space, and so is used for all the cases considered in the remainder of this paper (unless otherwise stated).

2.6. Validity of the CNS algorithm in physical space

The one-dimensional CGLE (5) is now used as an example to verify the validity of our CNS algorithms in physical space. First, the one-dimensional CGLE has closed-form plane-wave solutions [43,45,55,64] given by

$$A(x, t) = \sqrt{1 - q^2} e^{i(w_q t + q x)}, \tag{30}$$

where $w_q = c_3 - (c_3 + c_1) q^2$. Provided $c_1 c_3 < 1$, these solutions are linearly stable. Along the line $c_1 c_3 = 1$, the band of wave-vectors shrinks to zero corresponding to Benjamin-Feir or modulation instability of the uniform oscillatory solution [42,53]. Beyond Benjamin-Feir instability, when $c_1 c_3 > 1$, the system enters the phase chaos and defect chaos regimes.

To verify the CNS algorithm in physical space, as mentioned in Section 2.2, let us first consider the plane-wave solution (30) when $c_1 = 1.1$ and $c_3 = 0.2$, with the initial condition

$$A(x, 0) = \sqrt{1 - q^2} e^{i q x}, \tag{31}$$

in which $q = 8\pi/L$ and $L = 256$. Given that $c_1 c_3 < 1$, the solution should be in the form of (30) and linearly stable. We solve this problem by means of the two CNS algorithms using the same values of N , M , and N_s . As shown in Fig. 1, the numerical simulations produced by the two CNS algorithms agree well with the exact plane-wave solution (30) at $t = 500$. This verifies the validity of the two CNS algorithms in the spectral and physical spaces, described in Section 2.1 and Section 2.2.

Next, let us again consider the one-dimensional CGLE, but for the case $c_1 = 2$ and $c_3 = 1$, with the initial condition

$$A(x, 0) = \cos\left(\frac{4\pi x}{L}\right) + \cos\left(\frac{8\pi x}{L}\right) + i \cos\left(\frac{4\pi x}{L}\right). \tag{32}$$

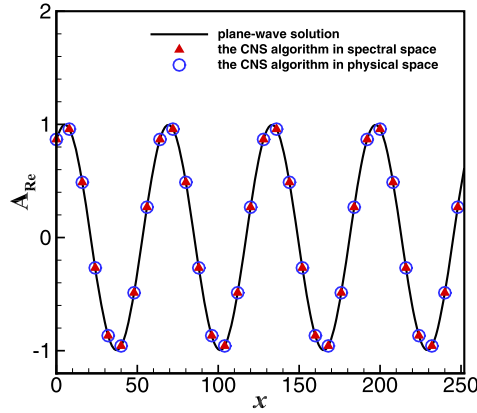


Fig. 1. Numerical simulations of the real part of $A(x, t)$ at $t = 500$ given by the two CNS algorithms using the mode-number $N = 64$ for the spatial Fourier expansion, the order $M = 8$ of temporal Taylor expansion and the number $N_s = 24$ of significant digits in multiple precision, compared against the exact plane-wave solution: plane-wave solution (solid line); result from CNS algorithm in spectral space (red symbols); and result from CNS algorithm in physical space (blue symbols).

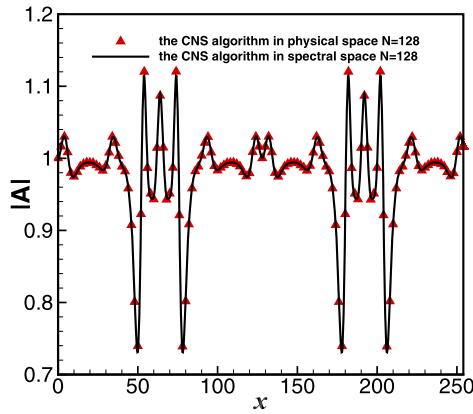


Fig. 2. Comparison of $|A(x, t)|$ profiles (at $t = 25$) obtained by the two CNS algorithms using the mode number $N = 128$ for the spatial Fourier expansion and the number $N_s = 24$ of significant digits in multiple-precision: converged results from the CNS algorithm in spectral space (solid line); and corresponding results from the CNS algorithm in physical space (red symbols).

Here $c_1 c_3 > 1$, and so the solution is unstable and becomes chaotic. The problem was solved using both CNS algorithms for $N = 128$ and $N_s = 24$. The results shown in Fig. 2 obtained using the two CNS algorithms are in close agreement with each other. This validates the CNS algorithm in physical space for problems involving the chaos regime.

Let $\tilde{A}(x, t)$ denote the numerical simulation for $c_1 = 2, c_3 = 1$ with the initial condition (32), given by the CNS algorithm in physical space with much smaller numerical noise by setting $N = 2048$. Hence, $\tilde{A}(x, t)$ can be regarded as much more accurate than the numerical simulations given by the two CNS algorithms in the spectral/physical space with $N = 128$. So, $\tilde{A}(x, t)$ can be used as a benchmark (or a reference solution). According to (26),

$$\delta(t) = \frac{\sqrt{\sum_{k=0}^{N-1} \left(\left| \tilde{A}(x_{16k}, t) \right| - |A(x_k, t)| \right)^2}}{\sqrt{\sum_{k=0}^{N-1} \left| \tilde{A}(x_{16k}, t) \right|^2}} \tag{33}$$

is the deviation of $|A(x_k, t)|$ (given by the CNS algorithm using $N = 128$) from the much more accurate simulation $|\tilde{A}(x, t)|$ (given by the same CNS algorithm using $N = 2048$). As shown in Fig. 3, the deviation $\delta(t)$ defined by (33) and the spectrum-deviation $\delta_s(t)$ defined by (28) of the numerical simulation $|A(x, t)|$ given by the CNS algorithm in physical space grow in a similar fashion to those given by the CNS algorithm in spectral space; in both cases, $N = 128$ and $N_s = 24$, with the reliability check using $N = 2048$ and $N_s = 24$.

The foregoing has shown that the CNS algorithm in physical space not only can greatly improve computational efficiency (see Section 2.5), but also can attain the same “critical predictable time” T_c as that of the CNS algorithm in the spectral space.

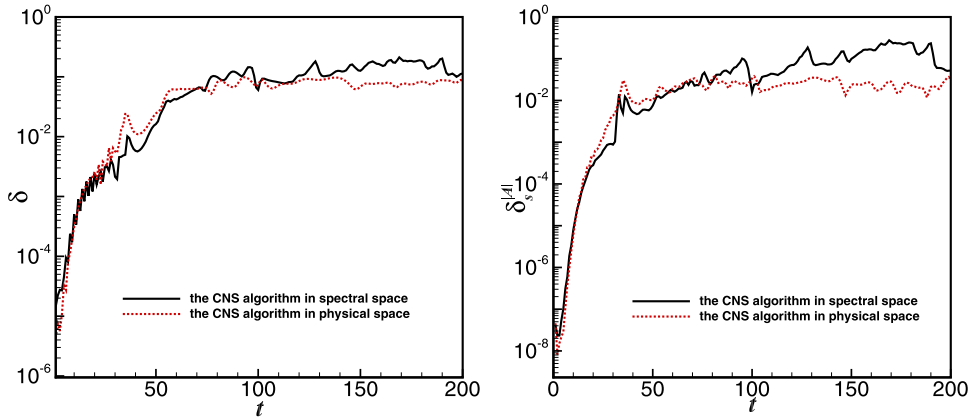


Fig. 3. Left: Comparison of the deviation $\delta(t)$ of $|A(x, t)|$ obtained by the two CNS algorithms using the mode number $N = 128$ for the spatial Fourier expansion and the number $N_s = 24$ of significant digits in multiple-precision, with reliability check using $N = 2048$ and the same N_s . Right: Comparison of the corresponding spectrum-deviation $\delta_s^{|A|}(t)$ of $|A(x, t)|$. Results given by the CNS algorithm in spectral space (black solid line); and by the CNS algorithm in physical space (red dashed line).

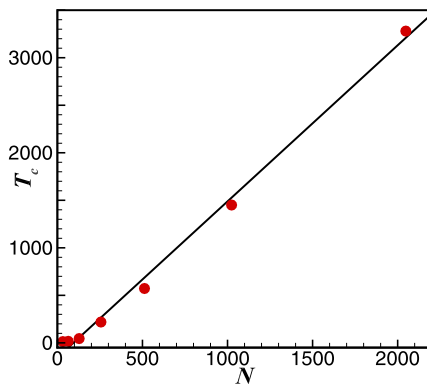


Fig. 4. Critical predictable time T_c versus the mode number N of the spatial Fourier expansion in a chaotic case of $c_1 = 2$ and $c_3 = 1$ with the initial condition (32), obtained by the CNS algorithm in physical space using the number $N_s = 105$ of significant digits in multiple-precision and different values of mode number N (from 32 to 2048). T_c given by the CNS (symbols); and analytic approximation formula (34) (solid line).

2.7. Relationship between T_c and the level of numerical noises

In summary, the basic idea of the CNS is to reduce the temporal/spatial truncation error and round-off error to such a required level that the computer-generated simulations are reliable throughout the entire spatial domain over a specified finite time interval $[0, T_c]$, where T_c is the critical predictable time. It is found that T_c is often dependent upon the level of numerical noises, dominated by the order M of temporal Taylor expansion, the mode number N of spatial Fourier expansion, and number N_s of significant digits in multiple-precision data for all variables and parameters. Thus, for a given critical predictable time T_c , we should choose sufficiently large values of M , N and N_s to guarantee such a reliable simulation in the whole spatial domain within $t \in [0, T_c]$. Given that a universal relationship between T_c and M , N , and N_s is unknown, it is often necessary to have to carry out an additional CNS simulation with even smaller noise in order to determine T_c in practice. Furthermore, because we have the freedom to choose the order M of the temporal Taylor expansion according to (25) for the optimal time-step, we need determine the relationship between T_c and N , N_s only. Here, let us again consider the one-dimensional CGLE for a chaotic case when $c_1 = 2$, $c_3 = 1$ with the initial condition (32) as an example to illustrate how to evaluate such kind of relationships.

To investigate the relationship between T_c and N , we first set $N_s = 105$ to guarantee that the round-off and temporal truncation errors are below a given threshold, noting that both errors are at the same level in the present CNS algorithm, whereby $tol = 10^{-N_s}$ (see Section 2.3). In this case, the spatial truncation error should be larger than other errors and thus make up the bulk of the numerical noise. Then, for the same problem, we alter N ($N = 2^n$ with n being a positive integer, in order to implement the FFT) from 32 to 2048 to obtain a series of CNS results at different levels of spatial truncation error, and then determine the corresponding critical predictable time T_c of each CNS result by comparing it with another CNS result using a larger N (and hence smaller spatial truncation error). Fig. 4 shows that the critical predictable time T_c in this case is almost directly proportional to N , such that

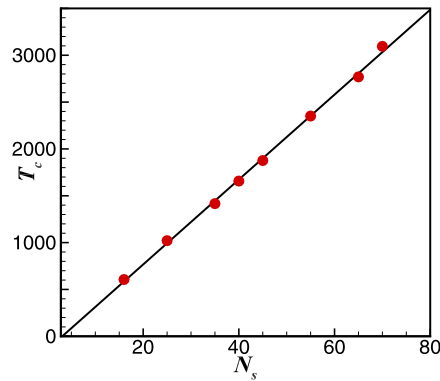


Fig. 5. Critical predictable time T_c versus the number N_s of significant digits in multiple precision in a chaotic case of $c_1 = 2$ and $c_3 = 1$ with the initial condition (32), given by the CNS algorithm in physical space using the mode number $N = 4096$ for the spatial Fourier expansion, the tolerance $tol = 10^{-105}$ for the temporal Taylor expansion and different values of N_s ranging from 16 to 70: T_c given by the CNS (symbols); and analytic approximation formula (34) (solid line).

$$T_c \approx 1.643 N - 154. \quad (34)$$

In addition, to investigate the relationship between T_c and N_s , we set mode number $N = 4096$ for the spatial Fourier expansion and the tolerance $tol = 10^{-105}$ for the temporal Taylor expansion and vary the number N_s of significant digits in multiple-precision from 16 to 70 with $10^{-N_s} > tol$ in order to ensure that the round-off error is the major source of numerical noise. In this way, for the same problem, we obtain a series of simulations given by the CNS, from which the corresponding critical predictable time T_c of each simulation is gained by comparing it against others with a larger N_s . Fig. 5 shows that the critical predictable time T_c is almost directly proportional to N_s in this case, such that

$$T_c \approx 45 N_s - 140. \quad (35)$$

Notably, when $N_s = 16$, corresponding to double precision, one has $T_c \approx 580$, say, using double precision, one can gain a reliable computer-generated simulation at most in $t \leq 580$, even if truncation error is very small by using a rather high order of temporal Taylor expansion and a rather large mode number N for the spatial Fourier expansion. This is exactly the same reason why high-order algorithms in double precision are useless for modifying convergence of chaotic computer-generated results, as previously mentioned by many researchers [2–5,7].

From (34) and (35), we have the linear relationship

$$T_c \approx \min \{1.643 N - 154, 45 N_s - 140\}. \quad (36)$$

Note that (36) provides an approximate relationship between T_c and N, N_s , which is important, although valid only for the case under consideration. Fortunately, it has been found that T_c is *always* directly proportional to N_s or N , approximately. Note that a similar linearity was reported by Turchetti et al. [31] about a chaotic map. So, this kind of linearity between T_c and N, N_s should exist in general. In practice, we can first gain such kind of linear relationship by means of relatively small values of N and N_s (corresponding to small values of T_c), and then further use this relationship to estimate the required (large) values of N and N_s for a given large value of T_c . In this way, the reliability check of the CNS simulation in a large interval of time may be avoidable, so that much CPU times is cut down.

According to (34) and (35), for the same T_c , the required value for the mode number N of spatial Fourier expansion grows faster than the required value for the number N_s of significant digits in multiple-precision. Thus, it is much more expensive and thus more challenging to obtain a reliable numerical simulation of a spatio-temporal chaotic system (governed by a nonlinear PDE) than a temporal chaotic one (by a set of nonlinear ODEs).

3. Influence of numerical noise on trajectories and statistics

It has been widely conjectured that long-term reliable computer-generated simulation of a chaotic system is impossible [2] even when the initial condition is exactly specified, because numerical noise from truncation and round-off errors inevitably occurs during each time-step of numerical simulation, and increases exponentially due to the butterfly-effect. Moreover, although *double* precision is widely used in computer-generated simulations, the influence of round-off error on reliable simulation of chaotic systems has been grossly underestimated. As several researchers have previously mentioned [3–5,7,20,21,33], it is *impossible* to achieve reliable, long-duration numerical simulations of chaotic systems by means of high-order algorithms in *double* precision. The importance of verification and validation (V & V) of computer-generated simulations is well known, and established techniques exist by which to determine the reliability of a numerical simulation (see e.g. [29,30]). The key point of the CNS is to ensure the reliability of computer-generated simulations: unlike traditional

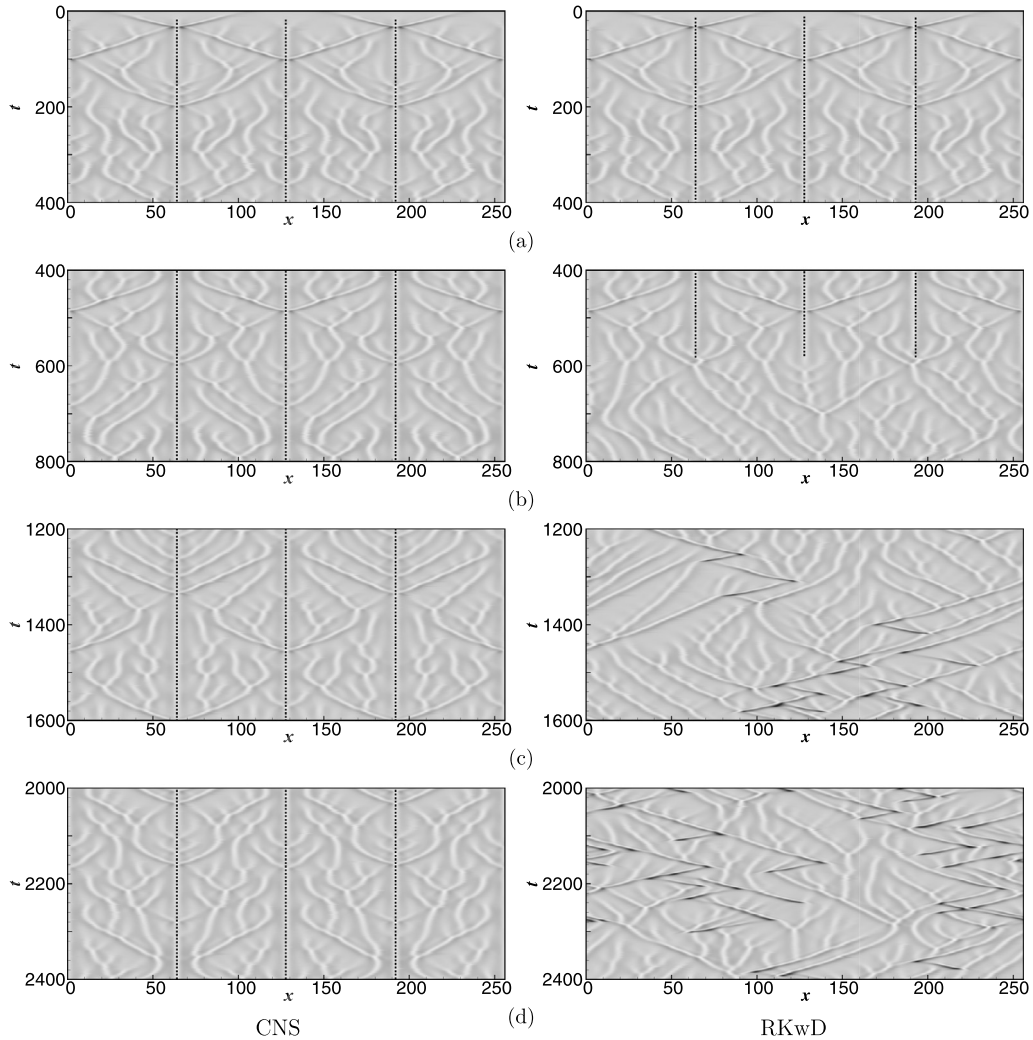


Fig. 6. Spatio-temporal plot of $|A(x, t)|$ using grey level representation from $|A| = 1.25$ (white) to $|A| = 0$ (black): (a) $0 \leq t \leq 400$; (b) $400 \leq t \leq 800$; (c) $1200 \leq t \leq 1600$; and (d) $2000 \leq t \leq 2400$. CNS results (left panels); and RKwD results (right panels).

algorithms, CNS acts to decrease *both* the truncation and round-off errors to a required level for reliable simulations of chaotic systems over a specified, large but finite interval of time, as illustrated by Liao and Wang [20,65] for the Lorenz equation. Therefore, the CNS can provide us reliable, convergent simulations of chaotic systems as benchmarks that make it possible to investigate the influence of numerical noise over a given interval of time by comparing these benchmarks with those produced by traditional algorithms in the *double* precision.

Without loss of generality, let us consider the one-dimensional CGLE within the chaotic regime when $c_1 = 2$ and $c_3 = 1$ for the same initial condition (32). In this case, the solution exhibits periodicity and symmetry in space. The reliable numerical simulations obtained by the CNS algorithm in physical space (marked as “CNS”) using $N_s = 105$ are used as benchmarks, which are compared with the corresponding results obtained by the temporal 4th-order Runge-Kutta method with double precision (marked as “RKwD”). Both the CNS and RKwD results have the same mode number $N = 4096$ for spatial Fourier expansion so that they have the same spatial truncation error. For time evolution, the CNS algorithm in physical space uses a high-order Taylor expansion with tolerance $tol = 10^{-105}$, whereas the RKwD utilises a time-step $\Delta t = 10^{-4}$ with associated temporal truncation error of order $O(10^{-16})$ (which is at the same level of the round-off error of the RKwD due to the use of double precision). According to (36), the CNS result (with $N_s = 105$ and $N = 4096$) has critical predictable time $T_c > 4500$, which is much larger than $T_c \approx 580$ for the RKwD simulation (with $N_s = 16$ and $N = 4096$). Notably, the CNS result is reliable over an interval of time about 7.7 times longer than that of the RKwD one. To guarantee the reliability, we use the CNS result in a smaller interval of time, say, $t \in [0, 3000]$, which therefore can be certainly used as a benchmark for comparisons described below.

Note that the initial condition (32) has a kind of spatial symmetry, which, according to the governing equation, should be retained by the solution (if evaluated correctly). As shown in Fig. 6, this is indeed true for the CNS result in the *whole*

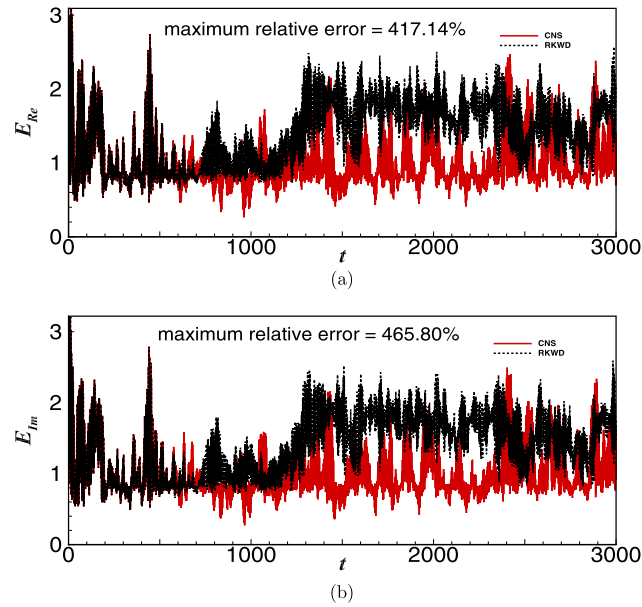


Fig. 7. Time histories of total spectrum-energy of the real and imaginary parts of the numerical simulations obtained by CNS and RKwD in the chaotic case of $c_1 = 2$ and $c_3 = 1$ with the initial condition (32): (a) real part, with maximum relative error 417.14%; and (b) imaginary part, with maximum relative error 465.80%. CNS results (red line); and RKwD results (black dashed line).

spatial domain $x \in [0, L]$ throughout the *entire* interval $t \in [0, 3000]$. However, the numerical simulation given by the RKwD loses the spatial symmetry at $t \approx 580$. For $t < 580$, the result given by the RKwD agrees quite well with that by the CNS. However, thereafter, the deviation between the two simulations becomes larger and larger, and the spatial symmetry in the RKwD result even breaks. This occurs mainly because, due to the butterfly-effect, numerical noise in the RKwD result increases exponentially. For $t > 580$, the RKwD result appears to become a mixture of the true solution and numerical noise at the *same* level of magnitude: as the numerical noise increases exponentially, the randomness in the noise first creates a distinct difference in the spatio-temporal trajectories and then causes a *spatial symmetry-breaking*. This indicates that numerical noise in the RKwD solvers might generate *not only* quantitative differences in the spatio-temporal trajectories *but also* some qualitative deviations in computer-generated simulation of chaotic system.

We now investigate the influence of numerical noise on the real and imaginary parts of the RKwD result, separately. At any given time, the result for each part can be expressed as a spatial Fourier expansion. Note that a spatial energy-spectrum of a spatio-temporal chaos at a given time often has important physical meanings. With this in mind, Fig. 7 depicts the comparison of the total spectrum-energy of the real and imaginary parts of the two simulations given by the CNS (in physical space) and RKwD, respectively. The two methods give almost the same total spectrum-energy when $t \leq 580$. However, thereafter, the deviation becomes increasingly distinct, with the maximum relative error reaching 417.14% for the real part and 465.80% for the imaginary part. The corresponding spectrum-deviation of the RKwD result (compared with the CNS one), defined by (28), becomes distinct after $t > 580$, with a maximum value of 551.23% for the real part and 603.83% for the imaginary part, as shown in Fig. 8. These results demonstrate that numerical noise can lead to great deviations not only in the spatio-temporal trajectories but also in the total spatial spectrum-energy of a chaotic system!

Why does numerical noise have such a huge influence on the total spectrum-energy of the real and imaginary parts of the RKwD simulation? To answer this question, let us compare the spatial Fourier spectra of the real part of the CNS and RKwD results at different times, as shown in Fig. 9. Note that, the odd wave numbers, i.e. $k = 1, 3, 5, \dots$, of the spatial Fourier spectra of the CNS result do *not* contain any energy at any stage throughout the *whole* interval of time $0 \leq t \leq 3000$. In other words, the odd wave number components of the spatial Fourier spectrum of the CNS result *always* remain zero. This is exactly the reason why the CNS results invariably retain the spatial symmetry over the entire time interval $0 \leq t \leq 3000$. However, this property of the true solution does not hold for the RKwD simulation. For small time, such as $t = 20$, the two spectra agree quite well. When $t = 600$, tiny differences can be discerned between the two spectra, and some odd wave number components in the spatial Fourier spectrum of the RKwD simulation have become energetic. Furthermore, Fig. 9 (c) and (d) show that as time increases, the deviation between the two spectra grows, and the odd wave number components in the spatial Fourier spectrum of the RKwD simulation contain an increasing amount of energy. At a sufficiently large time, such as $t = 1600$, the odd wave number components in the spatial Fourier spectrum of the RKwD simulation reach the *same* level of energy as the even components, as shown in Fig. 9 (d). This reveals a fundamental mistake in the RKwD simulation methodology. By comparing the spatial Fourier spectra (Fig. 10) of the imaginary part of the RKwD simulation with that of the CNS one, we reach the same conclusion. These results demonstrate that the random numerical noise of a chaotic system can rapidly increase to the *same* level (in both the real and imaginary parts) of the true solution and besides could transfer

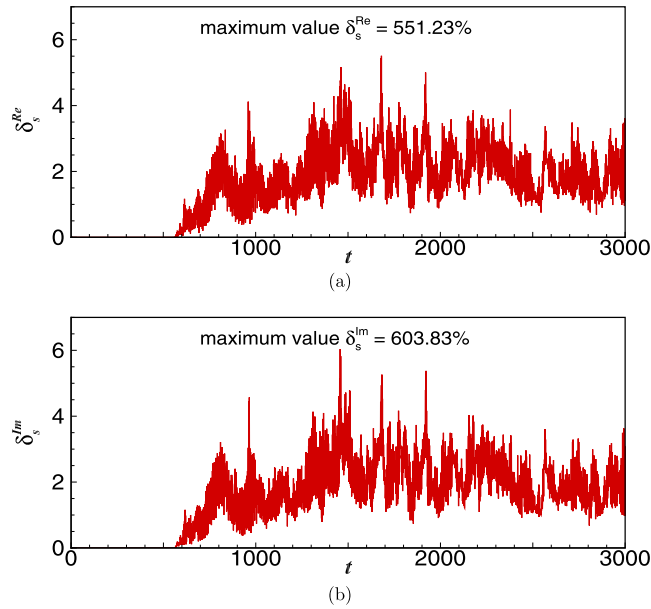


Fig. 8. Time histories of spectrum-deviation of the real and imaginary parts of the RKwD simulation in the chaotic case of $c_1 = 2$ and $c_3 = 1$ with the initial condition (32), compared with the benchmark given by CNS: (a) real part with maximum value $\delta_s^{Re} = 551.23\%$; and (b) imaginary part with maximum value $\delta_s^{Im} = 603.83\%$.

to all wave numbers of the spatial Fourier spectrum! The foregoing comparisons explain why the RKwD simulation might not only lose the spatial symmetry but also lead to great deviations in total spectrum-energy, and why numerical noise can lead to huge deviations in the spatio-temporal trajectories, the total spectrum-energy, and certain fundamental properties (such as spatial symmetry) of a chaotic system.

Fig. 11 presents a comparison between the spatial Fourier spectra of $|A(x, t)|$ obtained using the CNS and RKwD at different times. Again, the odd wave number components in the CNS spectrum contain no energy throughout the entire time interval, corresponding to the spatial symmetry of the true chaotic solution. At small times, such as $t = 20$, the two spectra are in close agreement. However, as time further increases, the odd wave number components in the spatial Fourier spectrum of $|A|$ obtained using RKwD amplify to the point at which they could reach the same energy level as the even components (Fig. 11 (b), (c) and (d)) at $t = 600$, $t = 1000$ and $t = 1600$. Again, this is incorrect, and is an artifact of numerical noise as it grows in the system as predicted by RKwD.

However, Fig. 12 indicates that $|A(x, t)|$ of the RKwD simulation has a maximum relative error 3.35% of the total spatial spectrum-energy with a maximum spectrum-deviation 20.99%, which are much smaller than those obtained above for the real and imaginary parts of $A(x, t)$. Note that $|A(x, t)|$ is a function of the real and imaginary parts of $A(x, t)$. It seems that the numerical errors of the real and imaginary parts of $A(x, t)$ might counteract each other for $|A(x, t)|$ in the case under consideration.

Note that the constant term in the spatial Fourier spectrum has the wave number zero, i.e. $k = 0$, corresponding to the overall spatial average of the simulation, and thus does not contain any information about the structure of the solution. In fact, it is the spatial Fourier spectrum without $k = 0$ that contains information on the solution structure. The spatial energy-spectrum without the wave number $k = 0$ of $|A(x, t)|$ obtained by the RKwD has a maximum relative error that is 735.99% of the total spatial spectrum-energy and a maximum relative error that is 803.54% of the spatial spectrum-deviation, as shown in Fig. 13. This reveals that numerical noise has a huge influence on the solution structure of $|A(x, t)|$ (as may be not evident in Fig. 12).

It is often assumed that numerical simulations of chaotic systems are sufficiently accurate in terms of their statistics even if their spatio-temporal trajectories are completely different. We now examine whether this is really true. First, let us compare the spatial mean value

$$\mu_{|A|}(t) = \frac{1}{L} \int_0^L |A(x, t)| dx$$

of $|A(x, t)|$ and the corresponding spatial standard deviation

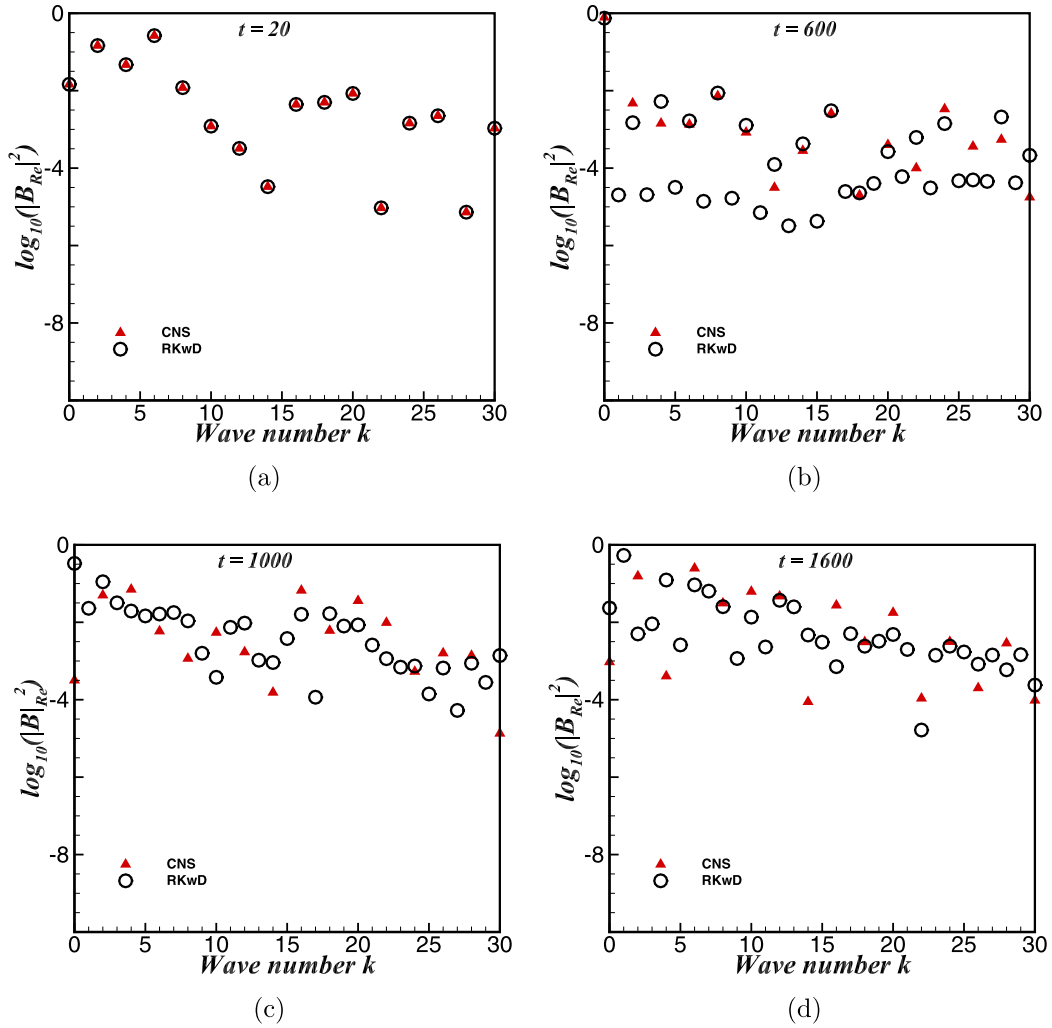


Fig. 9. Comparison of the spatial Fourier energy spectra of the real part of the computer-generated simulation obtained by the CNS and RKwD in the chaotic case of $c_1 = 2$ and $c_3 = 1$ with the initial condition (32): (a) $t = 20$; (b) $t = 600$; (c) $t = 1000$; and (d) $t = 1600$. CNS results (solid triangles); and RKwD results (open circles).

$$\sigma_{|A|}(t) = \sqrt{\frac{1}{L} \int_0^L [|A(x, t)| - \mu_{|A|}(t)]^2 dx},$$

of the CNS and RKwD results (using $N = 4096$) in the chaotic case of $c_1 = 2$ and $c_3 = 1$, subject to the initial condition (32). Fig. 14 shows that, for $t > 580$, the results given by RKwD are obviously different from those given by CNS, with a maximum relative error of 4.70% in the spatial mean $\mu_{|A|}(t)$ and 189.13% in the corresponding spatial standard deviation $\sigma_{|A|}(t)$. The differences grow considerably after $t > 1200$. This again confirms the deleterious effect of the contamination by numerical noise of computer-generated simulations of chaos even on the statistics, especially for long-duration simulations.

Secondly, let us examine the temporal mean

$$\mu_{|A|}(x) = \frac{1}{T} \int_0^T |A(x, t)| dt$$

and the corresponding temporal standard deviation

$$\sigma_{|A|}(x) = \sqrt{\frac{1}{T} \int_0^T [|A(x, t)| - \mu_{|A|}(x)]^2 dt}$$

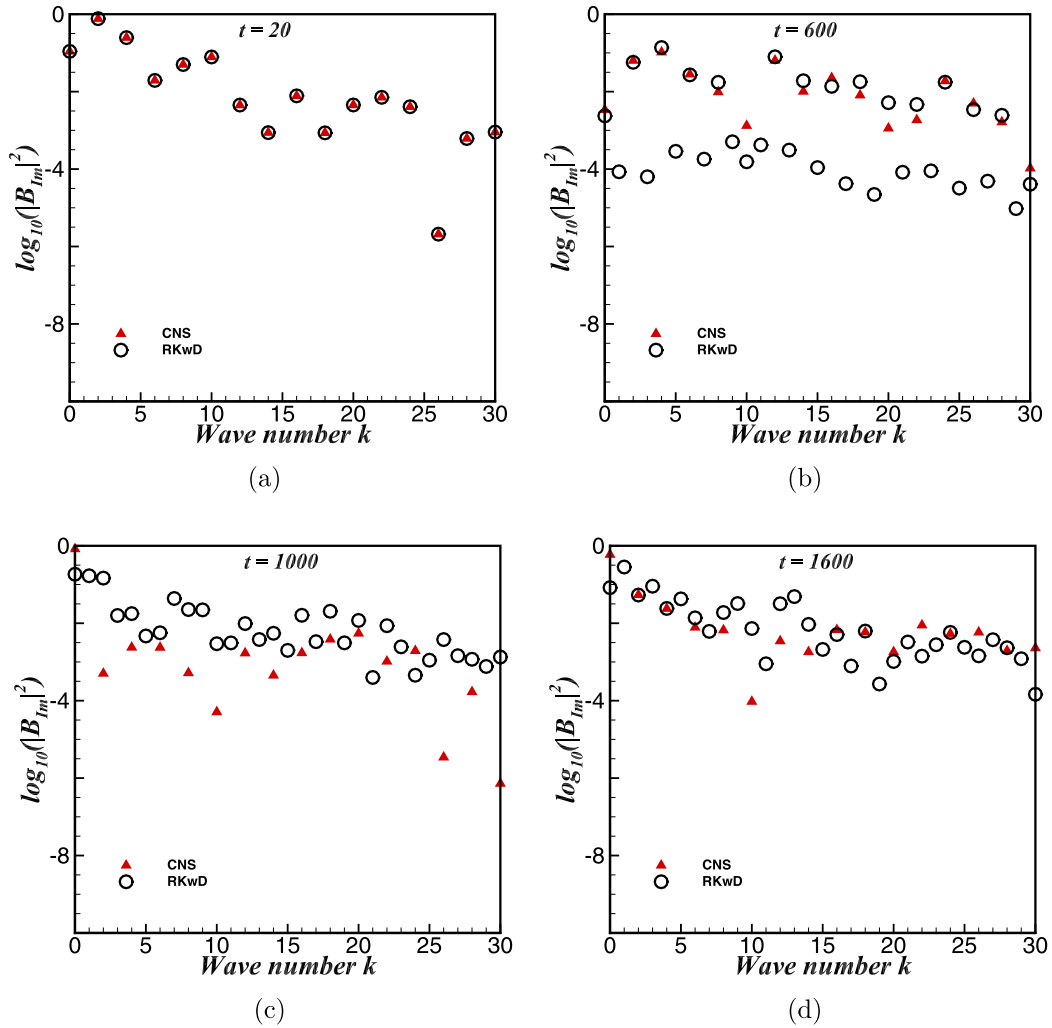


Fig. 10. Comparison of the spatial Fourier energy spectra of the imaginary part of the computer-generated simulations obtained by the CNS and RKwD in the chaotic case of $c_1 = 2$ and $c_3 = 1$ with the initial condition (32): (a) $t = 20$; (b) $t = 600$; (c) $t = 1000$; and (d) $t = 1600$. CNS results (solid triangles); and RKwD results (open circles).

of $|A(x, t)|$ given by the CNS and RKwD, where $T = 3000$. The temporal statistic results given by the RKwD exhibit obvious differences from those by the CNS, with a maximum relative error 9.88% in $\mu_{|A|}(x)$ and 536.05% in $\sigma_{|A|}(x)$, as can be seen in Fig. 15. Notably, although the temporal mean $\mu_{|A|}(x)$ and standard deviation $\sigma_{|A|}(x)$ obtained by the CNS have a kind of spatial symmetry, this fundamental statistical property of the true solution is lost in the RKwD simulation.

Turning thirdly to the spatial mean value

$$\mu_\varphi(t) = \frac{1}{L} \int_0^L \varphi(x, t) dx$$

of the phase $\varphi(x, t)$ of $A(x, t)$ and its corresponding spatial standard deviation

$$\sigma_\varphi(t) = \sqrt{\frac{1}{L} \int_0^L [\varphi(x, t) - \mu_\varphi(t)]^2 dx},$$

obtained by the CNS and RKwD results in the chaotic case of $c_1 = 2$ and $c_3 = 1$ with the initial condition (32). For $t > 580$, the results given by RKwD differ considerably from those given by CNS, with a maximum relative error of 1597139% and the maximum absolute error of 17.18 for the spatial mean $\mu_\varphi(t)$, maximum relative error of 1084.6% for the corresponding spatial standard deviation $\sigma_\varphi(t)$ (Fig. 16). The results continue to diverge for $t > 1200$. This again confirms the great impact

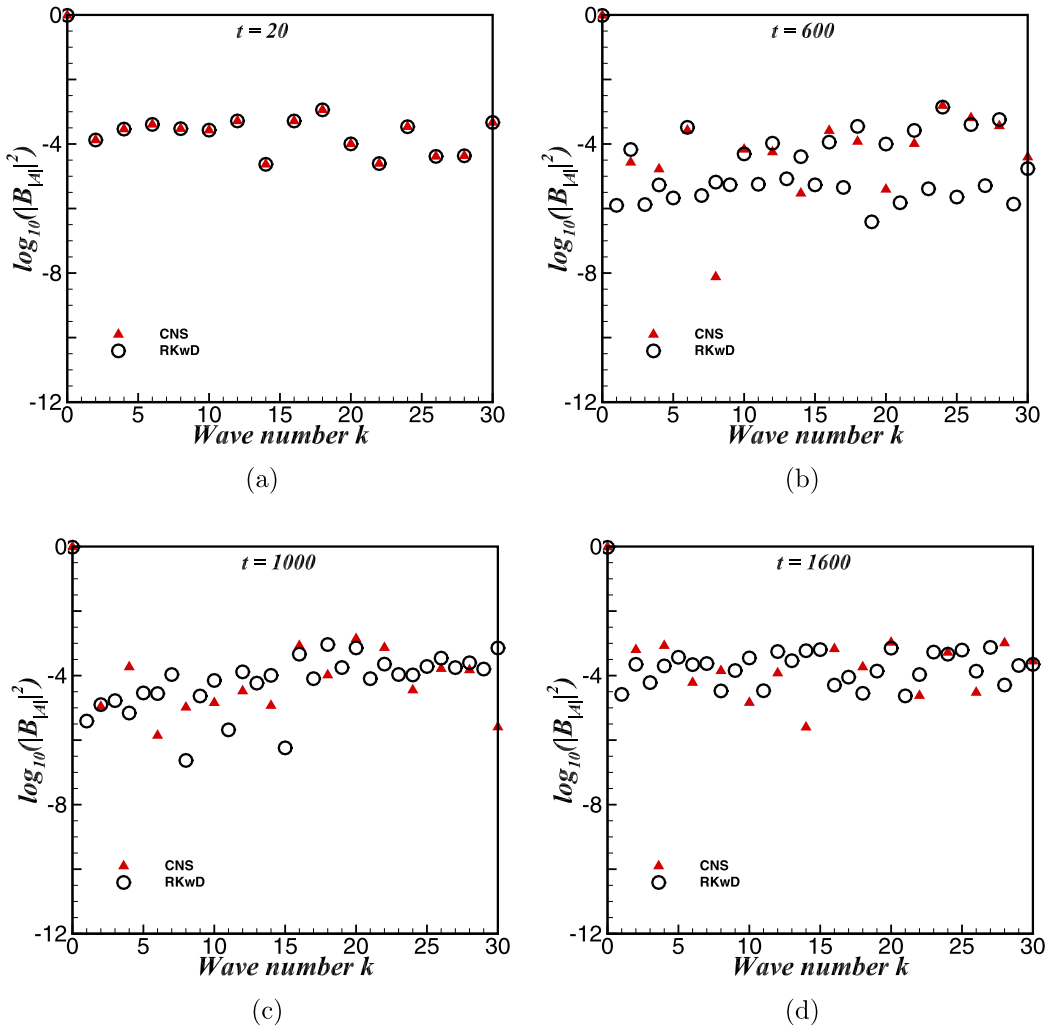


Fig. 11. Comparison of the spatial Fourier energy spectra of the computer-generated simulation $|A(x, t)|$ obtained by CNS and RKwD in the chaotic case of $c_1 = 2$ and $c_3 = 1$ with the initial condition (32): (a) $t = 20$; (b) $t = 600$; (c) $t = 1000$; and (d) $t = 1600$. CNS results (solid triangles); and RKwD results (open circles).

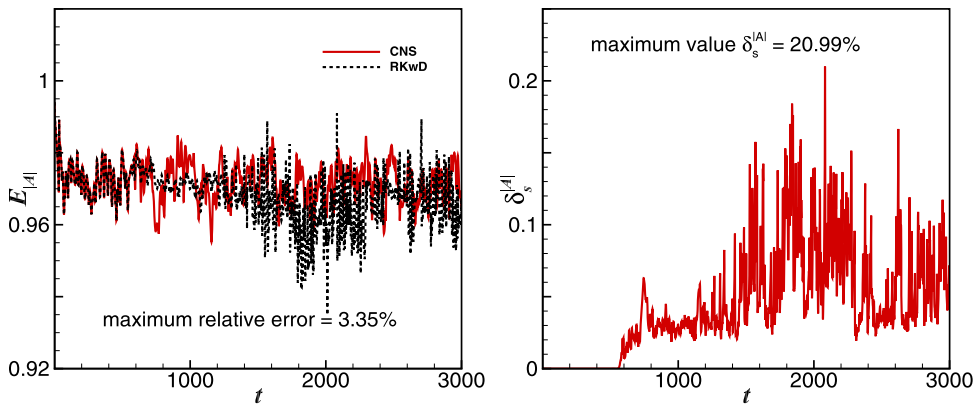


Fig. 12. Left: Time histories of total spectrum-energy of the computer-generated simulations $|A(x, t)|$ obtained by CNS and RKwD in the chaotic case of $c_1 = 2$ and $c_3 = 1$ with the initial condition (32): CNS result (red line); and RKwD result (black dashed line). Right: Time histories of corresponding spectrum-deviation $\delta_s^{|A|}$, with a maximum value of 20.99%.

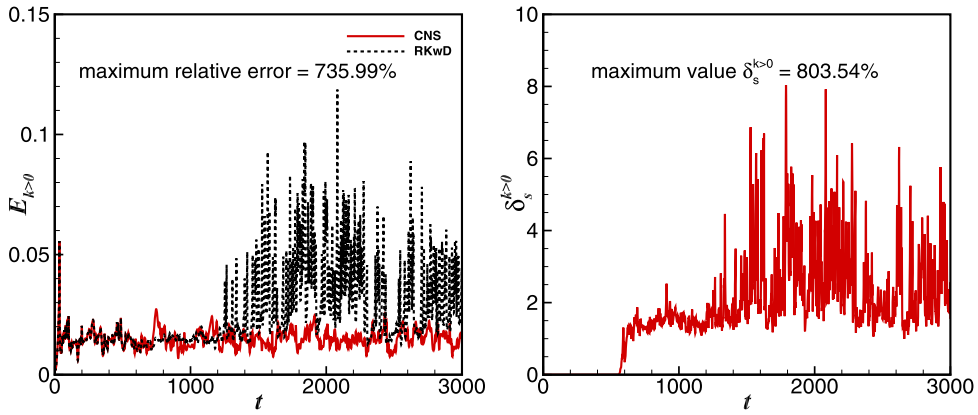


Fig. 13. Left: Time histories of spatial spectrum-energy $E_{k>0}$ of $|A(x, t)|$ except the zero wave number component, obtained by CNS and RKwD in the chaotic case of $c_1 = 2$ and $c_3 = 1$ with the initial condition (32), with a maximum relative error of 735.99%. CNS results (red line); and RKwD results (black dashed line). Right: Time histories of corresponding spectrum-deviation $\delta_s^{k>0}$ with a maximum value of 803.54%.

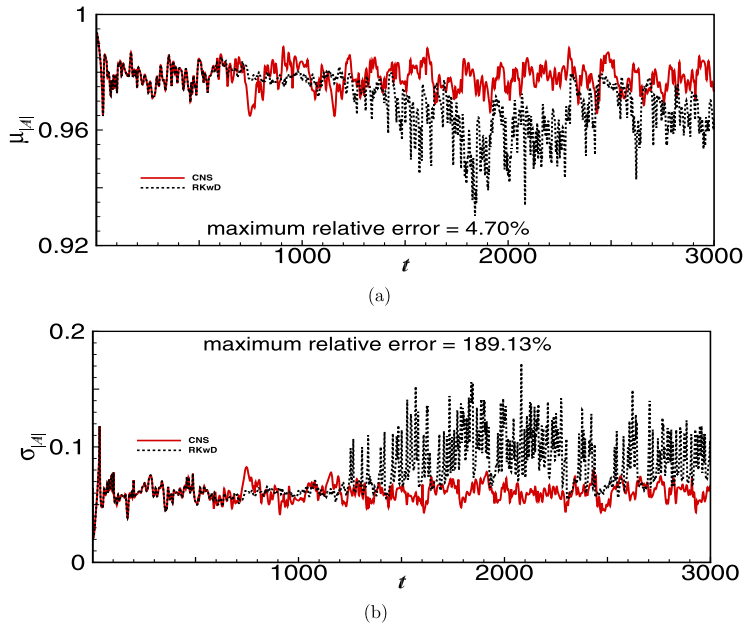


Fig. 14. Time histories of (a) spatial mean value $\mu_{|A|}(t)$ and (b) spatial standard deviation $\sigma_{|A|}(t)$ of $|A(x, t)|$ obtained by CNS and RKwD in the chaotic case of $c_1 = 2$ and $c_3 = 1$ with initial condition (32), with maximum relative errors of 4.70% for $\mu_{|A|}(t)$ and 189.13% for $\sigma_{|A|}(t)$, respectively: CNS results (red line); and RKwD results (black dashed line).

of numerical noise on computer-generated simulations of chaos *even* in terms of the statistics, particularly for long-duration simulations.

Next, we examine the temporal mean

$$\mu_\varphi(x) = \frac{1}{T} \int_0^T \varphi(x, t) dt$$

of the phase $\varphi(x, t)$ of $A(x, t)$ and its corresponding temporal standard deviation

$$\sigma_\varphi(x) = \sqrt{\frac{1}{T} \int_0^T [\varphi(x, t) - \mu_\varphi(x)]^2 dt},$$

where $T = 3000$. In Fig. 17 these temporal statistics of the RKwD numerical predictions display obvious differences from those by CNS, with maximum relative error of 857737% and maximum absolute error of 0.67 for $\mu_\varphi(x)$ and maximum

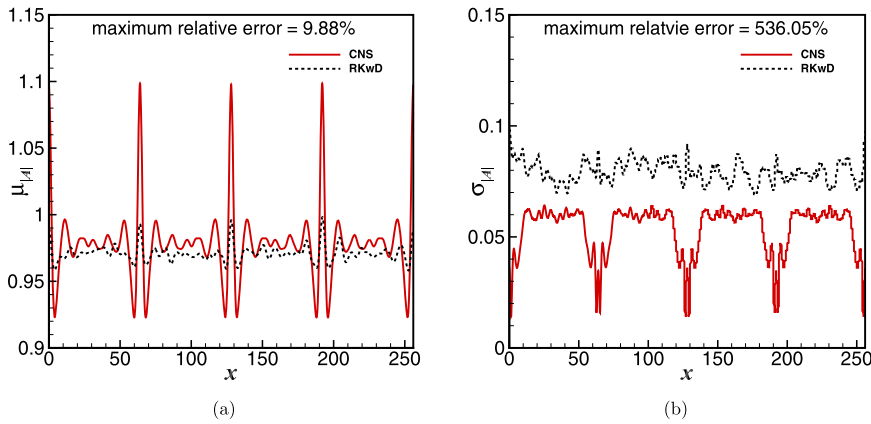


Fig. 15. Comparison of spatial profiles of (a) temporal mean $\mu_{|A|}(x)$ and (b) corresponding spatial standard deviation $\sigma_{|A|}(x)$ of $|A(x, t)|$, obtained by CNS and RKwD in the chaotic case of $c_1 = 2$ and $c_3 = 1$ with the initial condition (32), with maximum relative errors of 9.88% for $\mu_{|A|}(x)$ and 536.05% for $\sigma_{|A|}(x)$, respectively. CNS results (red line); and RKwD results (black dashed line).

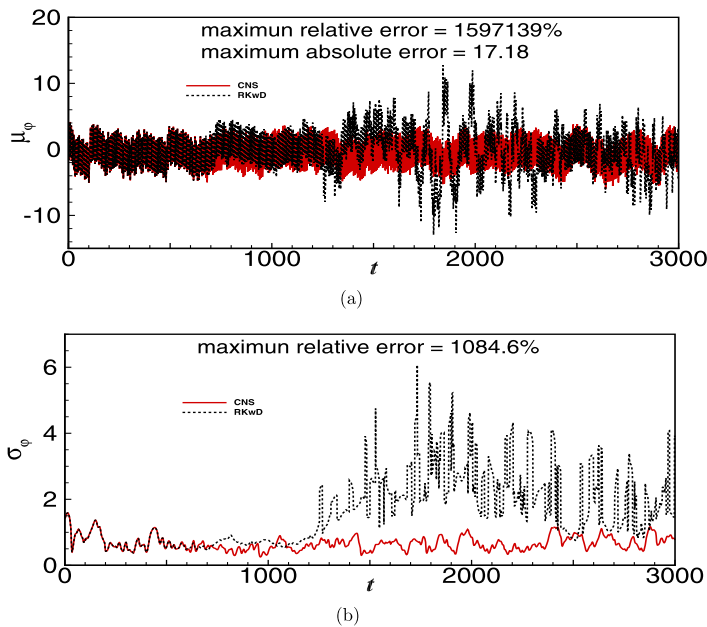


Fig. 16. Time histories of (a) spatial mean value $\mu_\varphi(t)$ and (b) spatial standard deviation $\sigma_\varphi(t)$ of phase of $A(x, t)$, obtained by CNS and RKwD in the chaotic case of $c_1 = 2$ and $c_3 = 1$ with the initial condition (32): CNS results (red line); and RKwD results (black dashed line).

relative error 166.53% for $\sigma_\varphi(x)$. The temporal mean $\mu_\varphi(x)$ and standard deviation $\sigma_\varphi(x)$ obtained by CNS again demonstrate a kind of spatial symmetry correctly, unlike the corresponding results from the RKwD simulations.

Fig. 16 shows that the spatial mean $\mu_\varphi(t)$ and the spatial standard deviation $\sigma_\varphi(t)$ of the CNS result remain similar throughout the entire interval $t \in [0, 3000]$. However, the corresponding RKwD results are highly non-stationary, with considerable changes between the values of spatial mean $\mu_\varphi(t)$ and spatial standard deviation $\sigma_\varphi(t)$ before and after $t \approx 1200$. Similar behaviour is exhibited by the spatial mean $\mu_{|A|}(t)$ and the spatial standard deviation $\sigma_{|A|}(t)$ shown in Fig. 14, the spatial spectrum energy of $|A|$ except the constant term (corresponding to the wave number $k = 0$) in Fig. 13, the total spectrum energy of $|A|$ in Fig. 12, and the total spectrum energy of the real and imaginary parts of $A(x, t)$ in Fig. 7.

The one-dimensional CGLE exhibits two distinct chaotic phases, namely “phase chaos” when A is bounded away from zero, and “defect chaos” when the phase of A exhibits singularities where $A \approx 0$, respectively [43,45,47]. Shraiman et al. [45] pointed out that the crossover between phase and defect chaos is invertible when $c_1 > 1.9$ (we consider $c_1 = 2$ in this section). Let

$$|A|_{min}(t) = \min \left\{ |A(x, t)| \mid x \in [0, L] \right\}$$

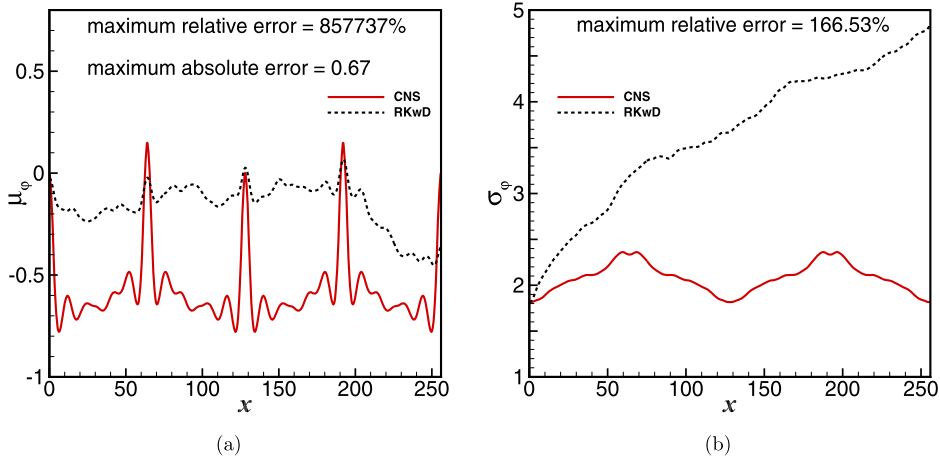


Fig. 17. Comparison of spatial profiles of (a) temporal mean $\mu_\phi(x)$ and (b) corresponding standard deviation $\sigma_\phi(x)$ of the phase of $A(x, t)$, obtained by CNS and RKwD in the chaotic case of $c_1 = 2$ and $c_3 = 1$ with the initial condition (32): CNS results (red line); and RKwD results (black dashed line).

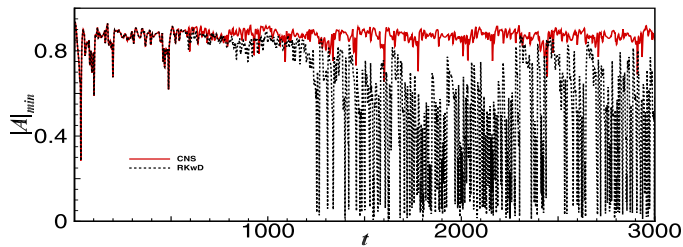


Fig. 18. Time histories of the spatial minimum of $|A(x, t)|$ obtained by CNS and RKwD over $t \in [0, 3000]$ in the chaotic case of $c_1 = 2$ and $c_3 = 1$ with the initial condition (32): CNS results (red line); and RKwD results (black dashed line).

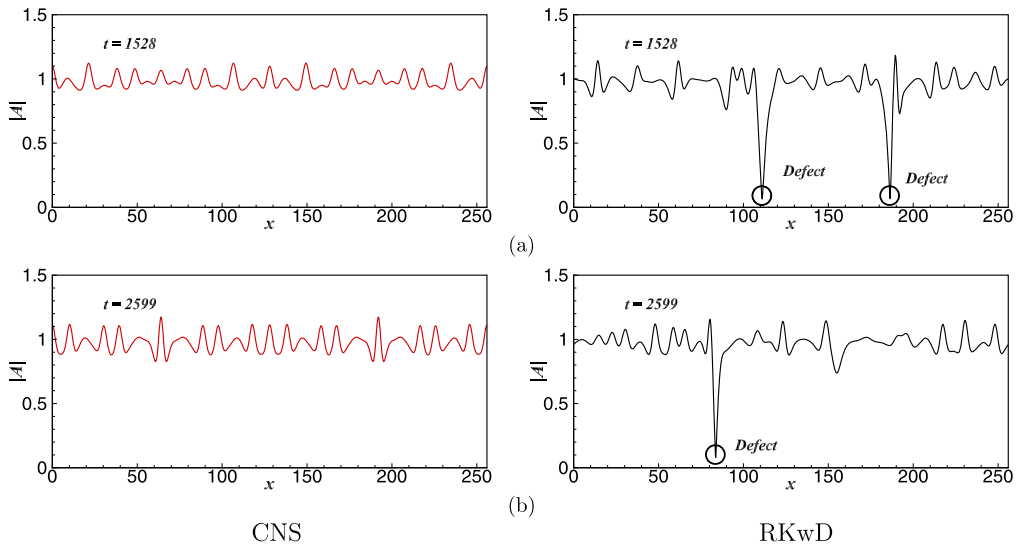


Fig. 19. Spatial profiles of $|A(x, t)|$ obtained by CNS and RKwD in the chaotic case of $c_1 = 2$ and $c_3 = 1$ with the initial condition (32): (a) $t = 1528$; and (b) $t = 2599$. Left: CNS results (red line); Right: RKwD results (black line).

denote the spatial minimum of $|A(x, t)|$ at a given time t . Fig. 18 compares time histories of $|A|_{min}(t)$ given by CNS and RKwD. It can be seen that the CNS result of $|A|$ is invariably bounded away from zero, implying that the solution is in the so-called *phase chaos* regime throughout the *entire* duration of the simulation, i.e. $t \in [0, 3000]$. However, the $|A|_{min}(t)$ given by RKwD often exhibits a sudden drop to a value very close to zero after $t > 1200$ (Fig. 18), corresponding to the so-called *defect chaos* displayed in Fig. 19 for $|A|$ and Fig. 20 for the phase ϕ with occasional jumps in phase indicating the

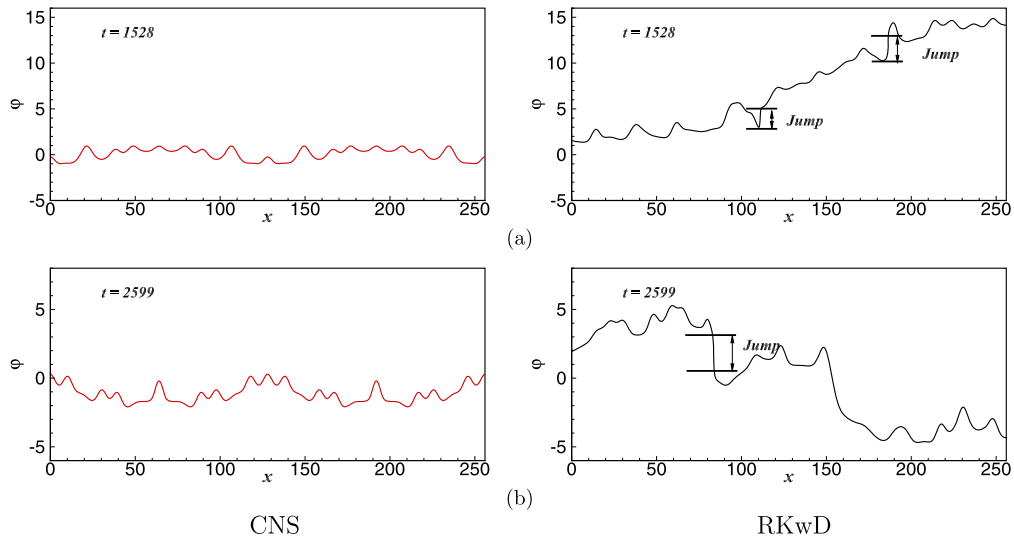


Fig. 20. Spatial profiles of the phase of $A(x, t)$ obtained by CNS and RKwD in the chaotic case of $c_1 = 2$ and $c_3 = 1$ with the initial condition (32): (a) $t = 1528$; and (b) $t = 2599$. Left: CNS results (red line); Right: RKwD results (black line).

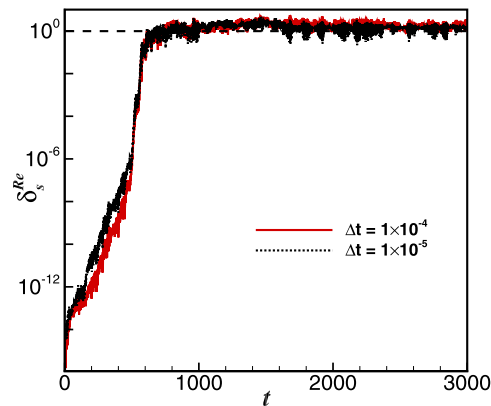


Fig. 21. Time histories of spectrum-deviation of the real part of the RKwD simulations in the chaotic case of $c_1 = 2$ and $c_3 = 1$ with the initial condition (32) using different values of time-step, with the CNS result as the benchmark: $\Delta t = 1 \times 10^{-4}$ (red solid line); and $\Delta t = 1 \times 10^{-5}$ (black dashed line).

presence of singularities. The RKwD simulation therefore *incorrectly* predicts a crossover between phase and defect chaos in the interval $[0, 3000]$, which does not occur in the *reliable* CNS result. This illustrates the risk posed by numerical noise in computer-generated simulation of chaotic systems.

Note that both of CNS and RKwD use the same number of modes, $N = 4096$, in the spatial Fourier expansion in space and thus have the same spatial truncation error. Given that CNS utilizes the temporal high-order Taylor series in multiple precision, the CNS algorithm should have a much smaller truncation error in time dimension than the 4th-order Runge-Kutta method in double precision (RKwD). It is found that using a smaller time-step (such as $\Delta t = 1 \times 10^{-5}$) can not improve the spectrum-deviations of the real part of $A(x, t)$ given by the RKwD, as evident in Fig. 21. This means that the temporal truncation error of RKwD is not the dominant source of its numerical noise. Instead, the numerical noise of the RKwD result primarily arises from the round-off error due to the use of double precision. So, all of the above-mentioned comparisons illustrate the risk of using double precision in computer-generated simulation of spatio-temporal chaotic systems, particularly for a long-duration simulation.

4. Concluding remarks and discussions

Due to the famous butterfly-effect, numerical noise caused by the truncation and round-off errors increases exponentially for chaotic system so that it is hard to obtain a reliable computer-generated simulation in a long-duration time. The shadowing method [9–14] works for a uniformly hyperbolic system, but hardly any chaotic systems are uniformly hyperbolic [15,16]. Particularly, there is no practical method to efficiently gain reliable computer-generated simulations in a long-duration time for spatio-temporal chaotic systems governed by nonlinear PDEs, to the best of our knowledge.

Unlike the shadowing method, the strategy of the Clean Numerical Simulation (CNS) is to greatly reduce numerical noises (caused by both of temporal/spatial truncation error and round-off error) to such a tiny level that is required for a reliable simulation in a given interval of time $t \in [0, T_c]$. Based on such a hypothesis that numerical noise of chaotic system increases exponentially, the so-called “critical predictable time” T_c is determined by comparing a simulation with an additional new one given by the same initial condition and physical parameters but smaller numerical noise. In this way, we gain a “clean” numerical simulation in $[0, T_c]$, whose noise is below a given criterion of noise. This kind of “clean” numerical simulation should be close to the true solution and thus can be used as a benchmark solution for many purposes, for example, verifying numerical results given by a developing code, studying the propagation of physical micro-level uncertainty of a chaotic dynamic system [21,35,38], finding new periodic orbits of the three-body problem [36,37,39], investigating the influence of numerical noise on chaotic simulations given by the traditional algorithms in double precision (as illustrated in this paper), and so on.

In this paper, a new CNS algorithm in physical space is proposed for spatio-temporal chaos, which is computationally much more efficient than its predecessor in spectral space [38]. To verify its computational performance, the new CNS algorithm was used to solve the one-dimensional complex Ginzburg-Landau equation (CGLE), a well known example of spatio-temporal chaos. In the case of $c_1 = 2$, $c_3 = 1$ with the initial condition (32), the CNS result (using the spatial Fourier mode number $N = 4096$ and the number $N_s = 105$ of significant digits in multiple precision) remained convergent over considerably long time interval $t \in [0, 3000]$ throughout the whole spatial domain $x \in [0, L]$, where $L = 256$. This CNS result was considered reliable, and was therefore used as a benchmark.

By comparing this benchmark solution with that obtained using the 4th-order Runge-Kutta integration in double precision (RKwD), it was found that the two simulations only exhibited agreement over a small interval of time $t \in [0, 580]$. The CNS solution retained a kind of spatial symmetry and the phase chaos over the entire time interval $t \in [0, 3000]$, unlike the RKwD simulation which lost the spatial symmetry when $t > 580$ and degenerated into a mixture of phase and defect chaos after $t > 1200$. Moreover, the odd wave number components in the spatial spectrum of the CNS benchmark solution invariably remained zero, i.e. did not attract energy, unlike the RKwD simulation where the odd wave number components progressively gained energy after $t > 580$. This energy transfer in the RKwD simulation has arisen as a consequence of the double precision arithmetic where random information at the level of the last significant figure has grown exponentially to the macroscopic level, contaminating all wave numbers in the spatial spectrum. Particularly, the RKwD simulation in a long-duration interval $t \in [0, 3000]$ is obviously different from the CNS result even in statistics! The overall message of this paper, based on the foregoing findings, is that numerical noise from truncation and round-off errors in double precision arithmetic could lead to huge quantitative and statistical discrepancies in predictions on spatio-temporal chaos.

It again should be noted that the Lorenz equation essentially derives from a greatly simplified form of the Navier-Stokes equations that are commonly used to describe turbulent flows. Given that chaos inherently has a close relationship to turbulence, it is important to check the risk posed by the use of double precision for numerical simulations of turbulent flows, particularly in a rather long interval of time.

Currently, the deep learning [66] has been widely used to many complicated problems including the turbulent flows [67,68] and the three-body problems [69]. What will happen when the deep learning is applied to solve spatio-temporal chaos whose statistic results are sensitive to numerical noises (as mentioned in this article)? This is an interesting but open question.

Since rather small truncation error is required in time dimension, a low order temporal algorithm is unacceptable in the frame of the CNS. For example, it is found that the standard low order method such as the third-order exponential time differencing (ETD) method [70,71], which is a straightforward extension of the 4th-order Runge-Kutta integration and can provide a rather long time step-size for stiff systems, requires a quite small time-step $\Delta t \approx 10^{-25}$ to obtain the reliable simulation in the time interval $t \in [0, 3000]$ for the considered problem. Its corresponding CPU time cost is too expensive.

Therefore, high order temporal algorithms must be considered in the frame of the CNS. Although the exponential time differencing (ETD) method also have high-order scheme of multi-step type [70,71], the high-order Taylor series method still has some irreplaceable advantages in practice. First, using the high-order Taylor series method is very convenient, because only initial condition is required for it. But using the multi-step type ETD is not easy, because a k th-order multi-step ETD requires k previous time step values. However, sufficiently accurate previous time step values are difficult to obtain, especially when the order k is high. In addition, this might bring additional numerical noise. Secondly, for the high-order Taylor series method, the code is the same for arbitrary order M . However, using the multi-step type ETD, one had to modify the code for a different order. This is rather inconvenient, especially when the required order is very high, as illustrated in [32]. Furthermore, according to our experience, the high-order Taylor series method seems more stable than the multi-step type ETD, especially when the order is rather high.

In this paper, a new CNS algorithm is proposed, which is based on the discretization of unknown variables in physical space, as illustrated in (16). The Fourier collocation method with the FFT is used to calculate the spatial partial derivatives only. As shown in §2.5, the new CNS algorithm in physical space is computationally much more efficient than its predecessor in spectral space described in §2.1. Besides, it gives as accurate simulation as its predecessor, as shown in §2.6. Since the new CNS algorithm directly solves problems in physical space, it is unnecessary for us to use the Fourier pseudo-spectral method [72,73], which is equivalent to the Fourier collocation method, as pointed by Peyret [61,62]. This also explains why the two CNS algorithms can give the simulations at the same level of accuracy, as shown in §2.6.

The CGLE has stiff solutions such as Bekki-Nozaki holes [74], and there exist isolated non-analyticities when defect chaos occur. Note that the so-called Bekki-Nozaki holes [74] has a closed-form solution, which is certainly *not* chaotic. However, in the case of $c_1 = 2$, $c_3 = 1$ with the initial condition (32), the CNS benchmark solution in $t \in [0, 3000]$ retains the “*phase chaos*”, because $|A|$ is *always* bounded away from zero, as shown in Figs. 18 and 19, and besides its phase has *no* jumps at all, as shown in Fig. 20. This is quite different from the RKwD simulation, whose $|A|$ often exhibits a sudden drop to a value very close to zero after $t > 1200$ (see Fig. 18), corresponding to the *defect chaos* displayed in Fig. 19 for $|A|$ and Fig. 20 for the phase φ with occasional jumps indicating the presence of *singularities*. Obviously, the singularity (related to the defect chaos) of the RKwD simulation is a kind of *artifact*, caused by the numerical noises and the butterfly-effect of chaos. Generally speaking, any singularities are difficult to solve numerically. So, it is worth investigating whether the CNS can handle such kind of singularities in spatio-temporal chaos, when they indeed exist.

According to our experience of the CNS on the Lorenz equation [20,32], the three-body problem [34–37,39], the Rayleigh-Bénard turbulent flows (governed by the Navier-Stokes equation) [38] and so on, a computer-generated simulation of a chaotic system often has a *finite* value of the critical predictable time T_c , which seems to be dependent upon values of physical parameters and level of numerical noises. From the viewpoint of the CNS, this is easy to understand, since numerical noise at a *specified* level needs, more or less, some time to propagate to a *critical* level, below which the simulation is *clean* and thus *reliable*. Obviously, the lower the *specified* level of the numerical noise, the larger the value of T_c , and besides, the lower the *critical* level of the noise, the more accurate and the more reliable is the CNS result. Here, T_c is determined by comparing two simulations, using the butterfly-effect of chaos (although it is traditionally often regarded to be negative). The CNS is generally valid for most of chaotic systems, even if they are *not* hyperbolic. So, compared to the shadowing lemma [9,10], the strategy of the CNS is more *practical*, though it loses somewhat mathematical rigour. Note that, using a simple model, Yuan and Yorke [75] showed that a numerical artifact may persist even for an arbitrary high numerical precision. Indeed, there is a long way to go to reach a reliable computer-generated simulation for any spatio-temporal chaotic systems in a reasonably long interval of time within a complicated spatial domain.

Declaration of competing interest

There is not any personal interest or relationship that has the potential to be affected by publication of the submitted manuscript.

Acknowledgement

Thanks to the anonymous reviewers for their valuable suggestions and constructive comments. This work is financially supported by the National Natural Science Foundation of China (Approval No. 91752104).

References

- [1] H. Poincaré, Sur le problème des trois corps et les équations de la dynamique, Acta Math. 13 (1) (1890) A3–A270.
- [2] E.N. Lorenz, Deterministic nonperiodic flow, J. Atmos. Sci. 20 (2) (1963) 130–141.
- [3] E.N. Lorenz, Computational chaos—a prelude to computational instability, Phys. D, Nonlinear Phenom. 35 (3) (1989) 299–317.
- [4] E.N. Lorenz, Computational periodicity as observed in a simple system, Tellus A 58 (5) (2006) 549–557.
- [5] J. Li, Q. Peng, J. Zhou, Computational uncertainty principle in nonlinear ordinary differential equations (i), Sci. China 43 (2000) 449–460.
- [6] J. Li, Q. Zeng, J. Chou, Computational uncertainty principle in nonlinear ordinary differential equations, Sci. China, Ser. E, Technol. Sci. 44 (1) (2001) 55–74.
- [7] J. Teixeira, C.A. Reynolds, K. Judd, Time step sensitivity of nonlinear atmospheric models: numerical convergence, truncation error growth, and ensemble design, J. Atmos. Sci. 64 (1) (2007) 175–189.
- [8] L. Yao, D. Hughes, Comment on “Computational periodicity as observed in a simple system” by Edward N. Lorenz (2006a), Tellus A 60 (4) (2008) 803–805.
- [9] D.V. Anosov, Geodesic flows and closed Riemannian manifolds with negative curvature, Proc. Steklov Inst. Math. 90 (1967) 3–210.
- [10] R. Bowen, ω -Limit sets for Axiom A diffeomorphisms, J. Differ. Equ. 18 (1975) 333–339.
- [11] S.M. Hammel, J.A. Yorke, C. Grebogi, Do numerical orbits of chaotic dynamical processes represent true orbits?, J. Complex. 3 (2) (1987) 136–145.
- [12] S.M. Hammel, J.A. Yorke, C. Grebogi, Numerical orbits of chaotic processes represent true orbits, Bull. Am. Math. Soc. 19 (2) (1988) 465–469.
- [13] C. Grebogi, S.M. Hammel, J.A. Yorke, T. Sauer, Shadowing of physical trajectories in chaotic dynamics: containment and refinement, Phys. Rev. Lett. 65 (13) (1990) 1527.
- [14] T. Sauer, J.A. Yorke, Rigorous verification of trajectories for the computer simulation of dynamical systems, Nonlinearity 4 (3) (1991) 961.
- [15] S. Dawson, C. Grebogi, T. Sauer, J.A. Yorke, Obstructions to shadowing when a Lyapunov exponent fluctuates about zero, Phys. Rev. Lett. 73 (14) (1994) 1927.
- [16] Y. Do, Y.-C. Lai, Statistics of shadowing time in nonhyperbolic chaotic systems with unstable dimension variability, Phys. Rev. E 69 (1) (2004) 016213.
- [17] T.D. Sauer, Shadowing breakdown and large errors in dynamical simulations of physical systems, Phys. Rev. E 65 (3) (2002) 036220.
- [18] V. Anishchenko, A. Kopeikin, J. Kurths, T. Vadivasova, G. Strelkova, Studying hyperbolicity in chaotic systems, Phys. Lett. A 270 (2000) 301.
- [19] W.B. Hayes, K.R. Jackson, A fast shadowing algorithm for high-dimensional ODE systems, SIAM J. Sci. Comput. 29 (4) (2007) 1738–1758.
- [20] S. Liao, On the reliability of computed chaotic solutions of non-linear differential equations, Tellus, Ser. A Dyn. Meteorol. Oceanogr. 61 (4) (2008) 550–564.
- [21] S. Liao, On the numerical simulation of propagation of micro-level inherent uncertainty for chaotic dynamic systems, Chaos Solitons Fractals 47 (2013) 1–12.
- [22] S. Liao, On the clean numerical simulation (CNS) of chaotic dynamic systems, J. Hydrodyn. Ser. B 29 (5) (2017) 729–747.
- [23] A. Gibbon, A program for the automatic integration of differential equations using the method of Taylor series, Comput. J. 3 (1960) 108.

- [24] D. Barton, I. Willers, R. Zahar, The automatic solution of systems of ordinary differential equations by the method of Taylor series, *Comput. J.* 14 (3) (1971) 243–248.
- [25] G. Corliss, D. Lowery, Choosing a stepsize for Taylor series methods for solving ODEs, *J. Comput. Appl. Math.* 3 (4) (1977) 251–256.
- [26] G. Corliss, Y. Chang, Solving ordinary differential equations using Taylor series, *ACM Trans. Math. Softw.* 8 (2) (1982) 114–144.
- [27] R. Barrio, F. Blesa, M. Lara, VSVO formulation of the Taylor method for the numerical solution of ODEs, *Comput. Math. Appl.* 50 (1–2) (2005) 93–111.
- [28] P. Oyanarte, MP - a multiple precision package, *Comput. Phys. Commun.* 59 (1990) 345–358.
- [29] W. Oberkampf, C. Roy, *Verification and Validation in Scientific Computing*, Cambridge University Press, 2010.
- [30] C. Roy, W. Oberkampf, A complete framework for verification, validation, and uncertainty quantification in scientific computing, in: 48th AIAA Aerospace Sciences Meeting Including the New Horizons Forum and Aerospace Exposition, 2010, p. 124.
- [31] G. Turchetti, S. Vaienti, F. Zanlungo, Asymptotic distribution of global errors in the numerical computations of dynamical systems, *Phys. A, Stat. Mech. Appl.* 389 (21) (2010) 4994–5006.
- [32] S. Liao, P. Wang, On the mathematically reliable long-term simulation of chaotic solutions of Lorenz equation in the interval $[0, 10000]$, *Sci. China, Phys. Mech. Astron.* 57 (2) (2014) 330–335.
- [33] S. Liao, Can we obtain a reliable convergent chaotic solution in any given finite interval of time?, *Int. J. Bifurc. Chaos* 24 (09) (2014) 1450119.
- [34] S. Liao, Physical limit of prediction for chaotic motion of three-body problem, *Commun. Nonlinear Sci. Numer. Simul.* 19 (3) (2014) 601–616.
- [35] S. Liao, X. Li, On the inherent self-excited macroscopic randomness of chaotic three-body systems, *Int. J. Bifurc. Chaos* 25 (09) (2015) 1530023.
- [36] X. Li, S. Liao, More than six hundred new families of Newtonian periodic planar collisionless three-body orbits, *Sci. China, Phys. Mech. Astron.* 60 (12) (2017) 129511.
- [37] X. Li, Y. Jing, S. Liao, Over a thousand new periodic orbits of a planar three-body system with unequal masses, *Publ. Astron. Soc. Jpn.* 70 (4) (2018) 64.
- [38] Z. Lin, L. Wang, S. Liao, On the origin of intrinsic randomness of Rayleigh-Bénard turbulence, *Sci. China, Phys. Mech. Astron.* 60 (1) (2017) 014712.
- [39] X. Li, S. Liao, Collisionless periodic orbits in the free-fall three-body problem, *New Astron.* 70 (2019) 22–26.
- [40] L. Crane, Infamous three-body problem has over a thousand new solutions, *New Scientist*, <https://www.newscientist.com/article/2148074-infamous-three-body-problem-has-over-a-thousand-new-solutions/>.
- [41] C. Whyte, Watch the weird new solutions to the baffling three-body problem, *New Scientist*, <https://www.newscientist.com/article/2170161-watch-the-weird-new-solutions-to-the-baffling-three-body-problem/>.
- [42] M.C. Cross, P.C. Hohenberg, Pattern formation outside of equilibrium, *Rev. Mod. Phys.* 65 (3) (1993) 851.
- [43] H. Sakaguchi, Breakdown of the phase dynamics, *Prog. Theor. Phys.* 84 (5) (1990) 792–800.
- [44] W. Schöpf, L. Kramer, Small-amplitude periodic and chaotic solutions of the complex Ginzburg-Landau equation for a subcritical bifurcation, *Phys. Rev. Lett.* 66 (18) (1991) 2316.
- [45] B.I. Shraiman, A. Pumir, W. van Saarloos, P.C. Hohenberg, H. Chaté, M. Holen, Spatiotemporal chaos in the one-dimensional complex Ginzburg-Landau equation, *Phys. D, Nonlinear Phenom.* 57 (3–4) (1992) 241–248.
- [46] T. Bohr, M.H. Jensen, G. Paladin, A. Vulpiani, *Dynamical Systems Approach to Turbulence*, Cambridge University Press, 2005.
- [47] L. Brusch, M.G. Zimmermann, M. van Hecke, M. Bär, A. Torcini, Modulated amplitude waves and the transition from phase to defect chaos, *Phys. Rev. Lett.* 85 (1) (2000) 86.
- [48] M. van Hecke, M. Howard, Ordered and self-disordered dynamics of holes and defects in the one-dimensional complex Ginzburg-Landau equation, *Phys. Rev. Lett.* 86 (10) (2001) 2018.
- [49] I.S. Aranson, L. Kramer, The world of the complex Ginzburg-Landau equation, *Rev. Mod. Phys.* 74 (1) (2002) 99.
- [50] P. Degond, S. Jin, M. Tang, On the time splitting spectral method for the complex Ginzburg-Landau equation in the large time and space scale limit, *SIAM J. Sci. Comput.* 30 (5) (2008) 2466–2487.
- [51] V. García-Morales, K. Krischer, The complex Ginzburg-Landau equation: an introduction, *Contemp. Phys.* 53 (2) (2012) 79–95.
- [52] Y. Uchiyama, H. Konno, Birth-death process of local structures in defect turbulence described by the one-dimensional complex Ginzburg-Landau equation, *Phys. Lett. A* 378 (20) (2014) 1350–1355.
- [53] T.B. Benjamin, J.E. Feir, The disintegration of wave trains on deep water Part 1. Theory, *J. Fluid Mech.* 27 (3) (1967) 417–430.
- [54] L. Brusch, A. Torcini, M. van Hecke, M.G. Zimmermann, M. Bär, Modulated amplitude waves and defect formation in the one-dimensional complex Ginzburg-Landau equation, *Phys. D, Nonlinear Phenom.* 160 (3–4) (2001) 127–148.
- [55] H. Chaté, Spatiotemporal intermittency regimes of the one-dimensional complex Ginzburg-Landau equation, *Nonlinearity* 7 (1) (1994) 185.
- [56] A. Torcini, Order parameter for the transition from phase to amplitude turbulence, *Phys. Rev. Lett.* 77 (6) (1996) 1047.
- [57] R. Montagne, E. Hernández-García, A. Amengual, M. San Miguel, Wound-up phase turbulence in the complex Ginzburg-Landau equation, *Phys. Rev. E* 56 (1) (1997) 151.
- [58] R. Montagne, E. Hernández-García, M. San Miguel, Winding number instability in the phase-turbulence regime of the complex Ginzburg-Landau equation, *Phys. Rev. Lett.* 77 (2) (1996) 267.
- [59] B.A. Finlayson, *The Method of Weighted Residuals and Variational Principles*, vol. 73, SIAM, 2013.
- [60] E. Isaacson, H.B. Keller, *Analysis of Numerical Methods*, Courier Corporation, 2012.
- [61] R. Peyret, Spectral methods for incompressible viscous flow, *Eur. J. Mech. B, Fluids* 22 (2) (2002) 199.
- [62] R. Peyret, *Spectral Methods for Incompressible Viscous Flow*, vol. 148, Springer Science & Business Media, 2002.
- [63] J.W. Cooley, J.W. Tukey, An algorithm for the machine calculation of complex Fourier series, *Math. Comput.* 19 (90) (1965) 297–301.
- [64] B. Janiaud, A. Pumir, D. Bensimon, V. Croquette, H. Richter, L. Kramer, The Eckhaus instability for traveling waves, *Phys. D, Nonlinear Phenom.* 55 (3–4) (1992) 269–286.
- [65] P. Wang, J. Li, Q. Li, Computational uncertainty and the application of a high-performance multiple precision scheme to obtaining the correct reference solution of Lorenz equations, *Numer. Algorithms* 59 (1) (2012) 147–159.
- [66] Y. LeCun, Y. Bengio, G. Hinton, Deep learning, *Nature* 521 (2015) 436–444.
- [67] M. Raissi, Z. Wang, M.S. Triantafyllou, G.E. Karniadakis, Deep learning of vortex-induced vibrations, *J. Fluid Mech.* 861 (2019) 119–137.
- [68] M. Raissi, A. Yazdani, G.E. Karniadakis, Hidden fluid mechanics: learning velocity and pressure fields from flow visualization, *Science* 367 (2020) 1026–1030.
- [69] P.G. Breen, C.N. Foley, T. Boekholt, S.P. Zwart, Newton versus the machine: solving the chaotic three-body problem using deep neural networks, *Mon. Not. R. Astron. Soc.* 494 (2020) 2465–2470.
- [70] S.M. Cox, P.C. Matthews, Exponential time differencing for stiff systems, *J. Comput. Phys.* 176 (2) (2002) 430–455.
- [71] G. Beylkin, J.M. Keiser, L. Vozovoi, A new class of time discretization schemes for the solution of nonlinear PDEs, *J. Comput. Phys.* 147 (2) (1998) 362–387.
- [72] L.N. Trefethen, Pseudospectra of matrices, *Numer. Anal.* 91 (1991) 234–266.
- [73] L.N. Trefethen, M. Embree, *Spectra and Pseudospectra: The Behavior of Nonnormal Matrices and Operators*, Princeton University Press, 2005.
- [74] N. Bekki, K. Nozaki, Formations of spatial patterns and holes in the generalized Ginzburg-Landau equation, *Phys. Lett. A* 110 (3) (1985) 133–135.
- [75] G. Yuan, J.A. Yorke, Collapsing of chaos in one dimensional maps, *Phys. D, Nonlinear Phenom.* 136 (1–2) (2000) 18–30.